Anonymous Referee #2

General Comments

This manuscript presents data of a flux experiment over a mixed oak and hornbeam forest. It focuses on VOCs measured by vDEC / PTR-QMS and presents some comparisons to EC / PTR-TOF measurements, which are presented in a companion paper under review in ACPD (Schallhart et al). The VOC flux experiment at the Bosco Fontana field site is part of a work package of the EU FP7 project ECLAIRE (http://www.eclaire-fp7.eu/). The authors intend to compare the measured canopy scale fluxes (topdown) of isoprene (and MT) with MEGAN modelled emission rates that are partly based on enclosure measurements. Such a closure would be an important goal for a study of this scale but the experimental design of the cuvette measurements (as far as this can be inferred from the manuscript) does not allow to attribute the gap between measured fluxes and modelled emissions to certain aspects of the model or the measurement (see specific comments on basal emission factors). The introduction outlines that flux measurements of BVOCs in a polluted region were carried out to study the interaction of natural and anthropogenic emissions and their interactions regarding air quality. This aspect would be of great interest to the readers of ACP and the scientific community but the authors do not make this connection at all. In its current form this manuscript is a description of VOC flux measurement with primary focus on technical aspects and exploratory data analysis (correlations, statistics) that may be basis of very valuable scientific insights but this connection to atmospheric chemistry (or the intent how this may be done based on this dataset) is missing.

Author response: We thank the referee for these helpful comments. The introduction has been modified to clarify the focus of this work. The authors feel that the experimental design of the cuvette system is justified (see response to specific comments below).

Specific Comments

Introduction

p29217 L10+: The Introduction relates average daily maximum concentrations measured in Modena. What does it mean if “the average daily maximum concentrations are peaking at 120mg

m-3" (the maximum is one data point with all other values of that day being lower. Over how many days were the maxima averaged and how can one value, i.e. the average, 'peak' at a certain value?) and how does that relate to the stated EU air quality legislation (how many exceedances where registered?). The authors mention the AQ standard 'for comparison' but the way in which the ozone situation is presented does not allow such a comparison.

Author response: This statement has been removed

Methods

The canopy height is stated as 28m in average. What is the range of tree heights in the vicinity of the tower? What is the roughness length and displacement height at the tower location? Why did the authors choose to measure at 32m on a 42m high tower, only 4m above the average canopy height? The authors need to demonstrate that the closeness to the canopy does not hamper the interpretation of the VOC fluxes (e.g. using turbulence data at the other tower levels).

There are various ways of defining the canopy height and 28 m is the height of the absolute maximum canopy elements and our measurement height and thus have mislead this reviewer a little. We chose the lower measurement height as a compromise to deal with fetch limitations (see also response to the question relating to the flux footprint below). Whilst the measurements were still in the surface roughness layer, this is typical for flux measurements over forests, with few flat forest areas sufficiently large to measure above. We did, however, mount a further sonic anemometer at 42 m height which allows us to investigate potential influences on either measurement height. Momentum fluxes agreed within 5% between measurement heights, but sensible heat fluxes were on average 15% larger at 32 m than at 42 m, independent of wind direction. The cause is unclear, also because the (two different types of) anemometers were not inter-compared during the campaign. Non-isotropic turbulence and fetch limitations would both be expected to have some wind direction dependence and it is hence difficult to decide which of the two measurements is the more accurate.

The tower seems to be a substantial structure likely causing significant flow disturbance. The sonic/inlet setup was situated at 32m on the NW corner of the tower, sampling a significant portion of the fluxes with the tower obstructing the atmospheric flow. The authors do not mention a data

QAQC criterion based on wind sectors. The authors either must demonstrate rigorously that the structural obstruction/setup does not affect the turbulence measurement or they must treat fluxes with a footprint from the disturbed sector with particular care (e.g. QAQC flag and exclusion from further analysis, compare turbulence parameters and VOC fluxes from disturbed vs undisturbed sector).

Author response: The impact of the tower on fluxes was assessed using the turbulent statistics and rotation angle used to realign measurements of u and w (θ). This assessment showed that the tower had little or no impact on fluxes so no QAQC flag was added. A discussion of this assessment has been added to the Supplementary Information.

There is no data QAQC criterion on whether a significant portion of the flux foot print was within the forest. This should be a standard criterion.

Author response: The percentage of flux files with > 25 % of the flux coming from outside of the forest area was found to be 26 %. This has been added to the Supplementary Information. As the flux footprint moves with atmospheric stability, these were mainly night-time conditions when emission rates are very small anyway.

To give the reader a better overview of the study site the authors should replace or extend Fig 2 by an average flux foot print density overlaid on a map of the forest.

Author response: Done

How long was the 1/8” Teflon line from the manifold to the PTR-QMS, what was the flow rate, pressure, residence time and Reynold’s number in that part of the inlet and how did this part contribute to the high frequency loss of the VOC measurements.

Author response: The 1/8” Teflon line was ~ 10 cm in length with a flow rate of 300 ml min^{-1} the Reynolds number was 258 with a residency time of 0.04 s. Unfortunately, we do not know the pressure in this line. These details have been added to the text.

p29220 L3+ : The authors state the QMS dwell time for VOC masses was 0.5 s. What is the response time (e.g. 95% rise time) of that particular instrument? Why did the authors choose relatively long dwell times when they could have increased the number of data points per 25 min period by reducing the dwell time with the benefit of reducing the high frequency loss associated with 0.5 s averaging? Also, in this paragraph the authors state there were ca 306 data points in each 25min period whereas on page 29223 L13 they say the typical number of measurement cycles, N, was 250 – which was it?

Author response: Shorter dwell times potentially provide better frequency response and an improved representation of the turbulence statistics, but they result in a noisier concentration time series that makes it harder to establish the accurate time lag (Langford et al., 2015) and also increase the overhead associated with m/z switching thus reducing overall measurement time for each m/z. The response time for this particular instrument has been assessed both during other field studies and in the laboratory, but not with the exact inlet configuration used in the field campaign. Our tests show the response time varies by compound, inlet length, temperature and humidity and to accurately quantify the response time would require a rise time (or decay rate) test for each half hour. The response time is about 0.5 s, recognising that the change in inlet configuration introduces some additional uncertainty. Thus, there is no benefit in using faster dwell times. In order to assess the impact of the response time on high frequency loss (averaged across the campaign) we have calculated the Horst correction factor for a response time of 0.25 s and 0.75 s, this gave a range of 0.94-0.97 indicating that reducing the dwell time would have a relatively minor effect on high frequency loss.

The correct number of data points in each 25 min averaging period is ca. 306. This has been corrected in the text.

p29221 L12+: The authors assume the calibration error was below 5%. This seems a very strong or boldly casual assumption – please, substantiate this claim. Do the authors have a traceable certificate that their gas standard itself has an accuracy of better than 5%? Did the authors calibrate the PTR-QMS at 1 ppm mixing ratios (in N2, dry) or may there be additional error associated with the dynamical dilution of the standard?

Author response: According to the supplier the gas standard itself has an accuracy of 5 % for isoprene, α-pinene and most other masses. However, we accept that there are likely to be additional errors introduced through dynamic dilution so we have increase the error stated in the text to 15 %.

With further regards to calibrations, how many calibrations where performed on the PTR-QMS? With the primary ion count ranging between 1.33 and 9 MHz and the water running out during the measurements the performance is expected to have changed throughout the experiment. How well did individual calibrations compare with each other (accuracy, repeatability)?

Author response: unfortunately, we don't have calibration data for the period immediately after the water running out but the instrument sensitivity at key masses varied little across the campaign. A summary of sensitives immediately before the campaign and at the campaign end are shown below for reference.

Compound	Sensitivity prior to campaign (ncps ppbv^{-1})	Sensitivity at campaign end (ncps ppbv^{-1})
methanol (*m/z* 33)	9.7	11.6
acetaldehyde (*m/z* 45)	11.9	9.9
acetone (*m/z* 59)	10.9	8.8
isoprene (*m/z* 69)	4.1	3.8
methyl ethyl ketone (*m/z* 71)	4.7	4.0

p29222: Eq.2 suggests that normalized product ion count rates were calculated from individual count rates of hydronium and water cluster ions measured at their respective 18O isotope masses, i.e. scaling factors of 500 and 250 respectively, for 0.2s (factor 5 to get to counting events). This might introduce unnecessary noise into the calculated mixing ratios. What is the measurement precision of the reported VOCs at typical mixing ratios (e.g. inferred from calibrations) based on the described method compared to calculating the concentrations based on averaged (e.g. running mean) primary ion counts?

Author response: Individual count rates were used to ensure that any spikes in the primary ion were corrected. Comparison of counts normalised using individual count rates and count rates calculated using a running mean showed very little difference with standard deviations across 200 points of 5.17 and 5.19 respectively. These values were calculated using isoprene calibration data.

p29224 L18+: Please, specify on which parameter(s) (c(t), w(t), <c',w'>,…) the stationarity test is based on.

Author response: The stationarity test is based on the flux <c',w'>. This has been clarified in the text.

Regarding leaf level emission measurements (p29226+) it is a misconception that basal VOC emission factors should be measured at one set of basal conditions of PAR (1000 mmol photons m-2 s-1) and leaf temperature (30C). This in fact renders the results of such efforts nearly useless with regards to upscaling as the parameter space is reduced from 2 dimensions to zero dimensions and the dependency of emissions on light intensity and temperature comes from the model rather than from the underlying measurements. A better strategy would be collecting emission rates at (near) ambient conditions for each leaf and calculating basal emission factors and PAR- and T-dependencies according to the parameterization of the used emission model. Also, the specific leaf area (leaf area per leaf mass for each species sampled) would be a valuable parameter to determine in such an effort. Sampling only leaves reachable from the ground is likely to result in a non-representative ensemble, as the authors state in the discussion (p29238, L10+). An experimental design that allows to put comprehensible error margins to the bottom-up and top-down approaches would further our scientific understanding, laborious speculation on the reasons for the discrepancies between the two less so. The concept of footprint and species dependent upscaling is innovative and interesting but the results are of limited substance. This reviewer, however, understands that the authors are using the data available and cannot go back in time to change the experimental design.

Author response: We very much agree with the reviewer's point that basal conditions should reflect ambient conditions and this was certainly the case in our study with midday temperatures typically ranging between 29 and 35 ºC (cf Fig. 1). The methodological approach to calculate BEF from leaves was the use of a Licor6400 equipped with a 6 cm^2 LED chamber connected to a cartridge. The cuvette does not allow measuring under ambient light condition. Although this can be reproduced with LED sensors, environmental conditions inside the cuvette are rarely well matched with ambient conditions outside the cuvette and multiple sun flecks which naturally occurs below the canopy does not help achieving steady state fluxes. Moreover, some time is needed to adapt the leaves to the enclosure conditions, therefore setting the cuvette light and temperature under basal conditions helps reaching a steady state condition of physiological parameters (we started sampling VOC emissions only when photosynthesis was stable). Another reason why we decided to measure under basal conditions is that it was to enable us to compare fluxes from different individuals per sample for statistical purposes. This would not be easy to do with varying fluxes measured under different conditions. Another reason why we measured under basal conditions, is that MEGAN model conventionally adopts Basal Emission Factors measured under basal conditions, we found several evidences of application of this approach in literature. Although SLA is a very valuable parameter (this may change between light and shade-adapted leaves), we found that in the version of MEGAN applied in this study this parameter had no use. We agree with the referee that measuring shade-adapted leaves was not an ideal condition to compare leaf emission with canopy-scale emissions, unfortunately it was not possible to reach upper layers of the canopy of the tree species of interest. We did our best however to reach leaves at the margin of canopies, so that they could be associated as much as possible to light-adapted leaves. A short explanation of this has been added to the text.

The discussion of monoterpene bottom-up vs top-down comparison (p29238, L17+) is strangely different from that of isoprene. Even though the upscaling of isoprene and MT emissions seem to have a similar skill, the discrepancy in the MTs is attributed to oxidation and deposition. The manuscript does not provide any evidence to which extent oxidation (what was the life time of the monoterpenes discussed) or deposition cause a discernable loss. The authors are encouraged to reconcile the two lines of argument and to replace speculations with tangible argumentation.

Author response: While it is unlikely that significant oxidation of isoprene occurs within the canopy, given the canopy air residence time, it is possible that monoterpenes could react. Gerosa et al. (manuscript in preparation) detected atmospheric concentration of ozone often exceeding 90 ppbv during light hours. The isoprene and monoterpene flux lost within the canopy at the Bosco Fontana field site has been investigated by Schallart et al. 2015. This study used measured values of ozone and NO_2 together with estimated OH and NO_3 values to estimate isoprene and monoterpene flux loss within the canopy. The isoprene flux loss reported was 3-5 % indicating that oxidation within the canopy had little impact upon isoprene fluxes. The monoterpene flux loss reported was 5-20 % indicating that up to 20 % of the monoterpene flux could be lost within the canopy. This discussion has been incorporated into the text.

Results

p29230 L8+: The agreement of isoprene fluxes of the two PTR instruments is classified as very good even though the slope is 1.3. Please, clarify whether this is the PTR-QMS over PTR-TOF data or vice versa and specify how the regression was calculated (orthogonal distance regression as necessary for two datasets that have a measurement error). The authors might want to add a scatter plot in Fig 4 that shows the regression results. Regarding Figure 4 this reviewer wonders why the MT flux data by PTR-QMS ends abruptly on June 25 whereas the isoprene fluxes from that same instrument continue after a one day gap. Please, clarify!

Author response: As suggested a scatter plot has been added to figure 4 clarifying the values reported on p29230 L8. The stop in the monoterpene measurements using the PTR-MS on June 25th was caused by a change to the nose cone voltage following a software crash. This change in voltage prevented meaningful measurements at high masses after this period.

p29231 and p29233: regarding the description of Fig7 this reviewer does not see a bimodal relationship in the mixing ratio scatter plot but it appears that the temperature effect is gradual and the regression of pairs of VOC mixing ratios shifts. This is particularly obvious in the MEK vs acetone plot with regressions shifting from low acetone (x-axis) intercepts to higher acetone intercepts with increasing temperature but with very similar slopes. The consideration of concentration ratios rather than regression slopes leads to the misinterpretation of the relationship between MEK and acetone. The argument how Fig7 suggests two distinct sinks or sources is not comprehensible. Please, clarify and rephrase. Please, keep in mind that the receptor site receives a big mix of air masses.

Author response: The authors believe that the consideration of concentration ratios is appropriate as this enables comparison with previous work (see p29233 line 23). This discussion has, however, been clarified and rephrased.

p29234 and Fig8: What is the purpose of fitting an exponential curve into the scatter plot of isoprene mixing ratios vs temperature (bottom panel)? The authors have no hypothesis for such a relation nor does the figure suggest one. The isoprene flux vs temperature plot (top panel) demonstrates that an exponential fit with temperature alone is a poor model for isoprene emissions as all the low/no light data cling to the zero emission line. This reviewer doubts that R2 in that exponential fit is 0.75 – please, clarify and consider skipping this exercise, substantiate it with scientifically sound reasons, or use a more comprehensive relationship.

Author response: As suggested the discussion of an exponential relationship between isoprene temperature and PAR has been reduced.

p29236 L3+: "In order to assess the effect of light on monoterpene emission the residual values from the temperature only model were plotted against PAR". Where? This is not shown.

Author response: This figure has been added

Supplement

Tab S1: The percentages of MeOH and acetaldehyde passing all tests is inconsistent with the failing of individual test aspects: MeOH failed the LOD criterion in 79% but is stated to pass all tests in 25% (>21%), which is logically impossible (acetaldehyde 18% > (100%-83%)). This reviewer agrees with the authors that VOC flux data should not be excluded per se from further analysis based on an LOD threshold (stated in the main text) since this may introduce a bias, but the authors must present their DAQC results in a consistent way (which portion of data went into which analysis and for what reasons where other portions excluded). Tab S1 and indeed the entire flux analysis is lacking either a criterion for undisturbed wind sectors or a rigorous demonstration that flow disturbances by the tower structure and the sonic do not impede the flux measurement.

Author response: The authors thank the review for noticing this issue, the values for the LoD criteria needed to be updated and have been corrected. The three quality tests were applied independently so all flux files underwent all three tests. The text has been clarified to make clear that data passing all tests and data falling below the LoD were included in all further analysis but any flux files failing the stationarity test or falling below the mean friction velocity (u*) threshold of 0.15 m s^{-1} were excluded from all further analysis. As discussed above an assessment of the impact of the tower on flux measurements has been added to the supplementary information.

Technical Comments

p29218 L6: The reservoir is to the north west of the tower location (45°11'51.0"N 10°44'31.0"E)

Author response: South West corrected to North West

p29228 L10+: The temperature varies by some 10 degrees and remains certainly not ‘more or less constant’ – please, avoid vague terminology and rephrase the description of the field site’s meteorology.

Author response: This has been corrected

Figure 1: Use dots or small markers for presenting the wind direction data as this allows to discern relative frequencies of certain wind sectors whereas lines just overcrowd the graph.

Author response: Done

p29230 L11: Add units to the intercept.

Author response: Done

The manuscript and Supplementary Information document with inserted text highlighted in green are displayed below.

Canopy-scale flux measurements and bottom-up emission estimates of volatile organic compounds from a mixed oak and hornbeam forest in northern Italy

Acton W. J. F. [1], Schallhart S. [2], Langford B. [3], Valach A. [1, 3], Rantala P. [2], Fares S. [4], Carriero G. [5], Tillmann R. [6], Tomlinson S. J. [3], Dragosits U. [3], Gianelle D. [7, 8], Hewitt C. N. [1] and Nemitz E. [3]

[1] {Lancaster Environment Centre, Lancaster University, Lancaster, LA1 4YQ, United Kingdom}

[2] {Division of Atmospheric Sciences, Department of Physics, University of Helsinki, Gustaf Hällströmin katu 2, 00560 Helsinki, Finland}

[3] {Centre for Ecology & Hydrology, Bush Estate, Penicuik, Midlothian, EH26 0QB, United Kingdom}

[4] {Research Centre for Soil-Plant System, Council for Agricultural Research and Economics, Rome, Italy}

[5] {Institute for Plant Protection CNR Research Area - Building E, Via Madonna del Piano 10, 50019 Sesto Fiorentino, Italy}

[6] {Institute of Energy and Climate Research, IEK-8: Troposphere, Research Centre Jülich, 52425 Jülich, Germany}

[7] {Sustainable Agro-ecosystems and Bioresources Department, Research and Innovation Centre, Fondazione Edmund Mach, 38010 S. Michele all'Adige, Italy}

[8] {Foxlab Joint CNR-FEM Initiative, Via E. Mach 1, 38010 San Michele all'Adige, Italy}

Correspondence to: E. Nemitz (en@ceh.ac.uk)

Abstract

This paper reports the fluxes and mixing ratios of biogenically emitted volatile organic compounds (BVOCs) 4 m above a mixed oak and hornbeam forest in northern Italy. Fluxes of methanol, acetaldehyde, isoprene, methyl vinyl ketone + methacrolein, methyl ethyl ketone and monoterpenes were obtained using both a proton transfer reaction-mass spectrometer (PTR-MS) and a proton transfer reaction-time of flight-mass spectrometer

(PTR-ToF-MS) together with the methods of virtual disjunct eddy covariance (PTR-MS) and eddy covariance (PTR-ToF-MS). Isoprene was the dominant emitted compound with a mean day-time flux of 1.9 mg m^{-2} h^{-1}. Mixing ratios, recorded 4 m above the canopy, were dominated by methanol with a mean value of 6.2 ppbv over the 28 day measurement period. Comparison of isoprene fluxes calculated using the PTR-MS and PTR-ToF-MS showed very good agreement while comparison of the monoterpene fluxes suggested a slight over estimation of the flux by the PTR-MS. A basal isoprene emission rate for the forest of 1.7 mg m^{-2} h^{-1} was calculated using the MEGAN isoprene emissions algorithms (Guenther et al., 2006). A detailed tree species distribution map for the site enabled the leaf-level emissions of isoprene and monoterpenes recorded using GC-MS to be scaled up to produce a “bottom-up” canopy-scale flux. This was compared with the “top-down” canopy-scale flux obtained by measurements. For monoterpenes, the two estimates were closely correlated and this correlation improved when the plant species composition in the individual flux footprint was taken into account. However, the bottom-up approach significantly underestimated the isoprene flux, compared with the top-down measurements, suggesting that the leaf-level measurements were not representative of actual emission rates.

1 Introduction

The term volatile organic compound (VOC) describes a broad range of chemical species emitted from natural and anthropogenic sources into the atmosphere. VOCs emitted from the biosphere are commonly termed biogenic VOCs (BVOCs). Of the BVOCs, isoprene is almost certainly the dominant species globally with an estimated annual emission of 535–578 × 10^{12} g C (Arneth et al., 2008; Guenther et al., 2012). Isoprene, along with larger terpenoids, are the BVOCs that have received the most attention in the literature to date. Although isoprene is the most commonly measured BVOC, global emission estimates of isoprene continue to differ and there are still large uncertainties associated with the emission estimates of many other compounds. For example annual monoterpene emission estimates vary between 32 × 10^{12} and 127 × 10^{12} g C (Arneth et al., 2008). A better understanding of how emissions change with land cover, temperature, soil moisture and solar radiation is required to constrain model descriptions of the effects of BVOCs on atmospheric chemistry in the past, present and future (Monks et al., 2009).

BVOCs are a major source of reactive carbon into the atmosphere and as such exert an influence on both climate and local air quality. BVOCs are oxidised primarily by the hydroxyl radical (OH), itself formed by the photolysis of ozone, to form peroxide radicals (RO_2). In the presence of NO_x (NO and NO_2) these RO_2 radicals can oxidise NO to NO_2, which may undergo photodissociation leading to the net formation of tropospheric ozone (Fehsenfeld et al., 1992). Tropospheric ozone can then impact human health, forest productivity and crop yields (Royal Society 2008; Ashmore 2005). In addition, BVOC species contribute significantly to the formation of secondary organic aerosol (SOA) in the atmosphere. This affects climate both directly and indirectly by the scattering of solar radiation and by acting as cloud condensation nuclei. The formation of cloud condensation nuclei leads to increased cloud cover and therefore an altering of the Earth's albedo (Hallquist et al., 2009).

The Bosco Fontana campaign was carried out as a part of the ÉCLAIRE (Effects of Climate Change on Air Pollution and Response Strategies for European Ecosystems) EC FP7 project to study the surface/atmosphere exchange within a semi-natural forest situated within one of the most polluted regions in Europe, and its interaction with air chemistry. During the Bosco Fontana campaign, VOC fluxes and mixing ratios were measured 4 m above the canopy of a semi-natural forest situated in the Po Valley, northern Italy (45° 11' 51" N, 10° 44' 31" E), during June and July 2012. The Po Valley experiences high levels of anthropogenic pollution caused by its proximity to the city of Milan's high levels of industrial and traffic-related emissions of pollutants, intensive agriculture and periods of stagnant air flow caused by the Alps to the north and west and the Apennines to the south (Bigi et al., 2011; Decesari et al., 2014).

Here we report the fluxes and mixing ratios of a range of BVOCs recorded from mixed mesophile forest at the Bosco Fontana field site. We compare BVOC flux calculation from above canopy eddy covariance measurements using both a proton transfer reaction-mass spectrometer (PTR-MS) and a proton transfer reaction-time of flight-mass spectrometer (PTR-ToF-MS) with isoprene and monoterpene fluxes obtained by scaling up leaf-level emission data to produce a canopy-scale "bottom-up" modelled flux estimate. We further explore the potential of accounting for the spatial tree species distribution for improving the comparison between top-down and bottom-up approaches.

2 Methods

2.1 Site description

Measurements were taken at a site within the Bosco Fontana natural reserve (45° 11' 51" N, 10° 44' 31" E), a 233 ha area of semi-natural woodland situated in the municipality of Marmirolo in the Po Valley. The forest canopy had an average height of approximately 28 m and was principally comprised of *Carpinus betulus* (hornbeam) and three oak species *Quercus robur* (pedunculate oak), *Quercus cerris* (turkey oak) and the introduced *Quercus rubra* (northern red oak) (Dalponte et al., 2007). In the centre of the forest there was a cleared area containing a seventeenth century hunting lodge surrounded by hay meadows. The surrounding area was predominantly arable farm land with some pastures to the north and west and a reservoir to the north west. The city of Mantova lies approximately 5 km to the south east, with the small towns of Marmirolo, Soave and Sant'Antonio approximately 2 km north, 1 km west and 3 km east, respectively. A 42 m measurement tower was situated near the centre of the forest to the south west of the central hay meadows. The measurement tower was ca.760 m from the edge of the forest in the direction of the easterly wind direction that dominated during this measurement period.

2.2 PTR-MS and PTR-ToF-MS setup and measurement procedure

In order to record BVOC fluxes and concentrations, both a high sensitivity PTR-MS (Ionicon Analytik GmbH, Innsbruck, described in detail by Blake et al., 2009; de Gouw and Warneke 2007; Hansel et al., 1995; Lindinger et al., 1998) and a high resolution PTR-ToF-MS (Ionicon Analytik GmbH, Innsbruck, as described by Graus et al., 2010; Jordan et al., 2009) were used, together with a sonic anemometer (Gill HS, Gill Instruments Ltd, UK). The PTR-MS was equipped with a quadrupole mass analyser and three turbo molecular pumps (Varian). The Silcosteel inlet and internal tubing were heated to avoid condensation of BVOCs onto internal surfaces. The application of PTR-MS to atmospheric measurements has previously been described by Hewitt et al. (2003) and Hayward et al. (2002).

The sonic anemometer was situated 32 m above the ground on the north-west corner of the tower. Both the PTR-MS and the PTR-ToF-MS were housed in an air-conditioned cabin at the base of the tower. The PTR-MS sub-sampled via a ca. 10 cm, 1/8 inch (O.D.) PTFE tube (I.D.: 1 mm, flow rate: 300 ml min^{-1}, residence time: 0.04 s and with a Reynolds number inside the tube of 258) from a ½ inch O.D. PTFE common inlet line (I.D. 3/8 inch), heated to avoid condensation, which led from ca.10 cm below the sonic anemometer to the cabin. Solenoid valves were used to switch between the sample line and zero air which was generated by passing ambient air through a glass tube packed with platinum catalyst powder heated to 200°C. The PTR-ToF-MS subsampled via a 3-way valve from the common inlet line; 0.5 L min^{-1} was pumped through a 1/8 inch (O.D.) and 1/16 inch (O.D.) capillary (together ca. 20 cm long), with 30 ml min^{-1} entering the instrument and the remaining flow being sent to an exhaust. The common inlet line had a flow rate of ca. 63 L min^{-1}, giving a Reynolds number of ca. 9700 which indicates a turbulent flow. There was no observable influence of the high flow rate on readings from the sonic anemometer, even during periods of relatively low turbulence. Data from both the PTR-MS and the sonic anemometer were logged onto a laptop using a program written in LabVIEW (National Instruments, Austin, Texas, USA).

The PTR-MS was operated continuously throughout the measurement campaign with pauses for optimising the instrument and refilling the water reservoir. PTR-MS settings were controlled so that the reduced electric field strength (E/N, where E is the electric field strength and N the buffer gas density) was held at 122 Td (1.22×10^{-19} V m^{-2}), with drift tube pressure, temperature and voltage maintained at 2.1 mbar, 45 °C and 550 V respectively. The primary ions and the first water cluster were quantified indirectly from the isotope peaks at m/z 21 ($H_2{}^{18}O^+$) and m/z 39 ($H_2{}^{18}O.H_2O^+$), respectively. The inferred count rate of H_3O^+ ions over the course of the campaign varied between 1.33×10^6 and 9.00×10^6 counts s^{-1}. O_2^+ (m/z 32) was kept below 1 % of the primary ion count throughout the campaign in order to limit ionisation of VOCs through charge transfer reactions with O_2^+ and minimise the contribution of the O_2^+ isotope ($^{16}O^{17}O^+$) to m/z 33.

During PTR-ToF-MS operation the drift tube temperature was held at 60°C with 600 V applied across it. The drift tube pressure was 2.3 mbar resulting in an E/N of 130 Td. A more detailed description of the PTR-ToF-MS operation is provided by Schallhart et al. (2015).

The PTR-MS was operated in three modes; the instrument measured zero air for 5 min, followed by 25 min in flux mode, 5 min in scan mode and then a final 25 min in flux mode. While in flux mode, 11 protonated masses were monitored sequentially: m/z 21 the hydronium ion isotope, m/z 39 a water cluster isotope and 9 masses relating to VOCs: m/z 33, 45, 59, 61, 69, 71, 73, 81 and 137. The mass spectral peaks at *m/z* 21 and 39 were analysed with a 0.2 s dwell time (τ). For the nine VOC species τ = 0.5s was used in order to increase the instrumental sensitivity to these masses. This gave a total scan time of 4.9 s and the acquisition of ca. 306 data points in each 25 min averaging period. The uncertainty caused by disjunct sampling was calculated and found to cause a 0.17 % error in the flux estimation (see Supplementary Information for details).

Identification of the compounds observed at each of these masses is complicated by the fact that PTR-MS only allows the identification of nominal masses, therefore it is impossible to distinguish between isobaric compounds. As such there may be more than one compound contributing to each of the measured masses; Table 1 displays the masses monitored and the compounds likely to be contributing to each mass together with the exact masses observed at each unit mass using the PTR-ToF-MS which has much greater mass resolution than does the quadrupole PTR-MS instrument. It was assumed that the dominant contributions at *m/z* 33, 45, 59, 61, 69, 71, 73, 81 and 137 were from protonated methanol, acetaldehyde (ethanal), acetone (propanone), acetic acid (ethanoic acid), isoprene (2-methyl-1,3-butadiene), methyl vinyl ketone (MVK, butenone) and methacrolein (MACR, 2-methylprop-2-enal), methyl ethyl ketone (MEK, butanone), a monoterpene mass spectral fragment and monoterpenes respectively. A further contribution to *m/z* 71, recently identified, are isoprene hydroxy hydroperoxides (ISOPOOH, Rivera-Rios et al., 2014). However, the concentrations of this intermediate are small if NO_x concentrations are high and therefore are likely to be negligible at this site, where NO_x concentrations were large (A. Finco, personal communication, 2015).

2.2.1 PTR-MS calibration

The PTR-MS was calibrated using a gas standard (Ionicon Analytic GmbH, Innsbruck) containing 17 VOCs at a mixing ratio by volume of approximately 1 x 10^{-6} (ca. 1 ppmv). The protonated mass of the VOCs ranged from *m/z* 31 (formaldehyde, CH_3O^+) to *m/z* 181 (1,2,4-trichlorobenzene, $C_6H_4Cl_3^+$). Methanol (*m/z* 33), acetaldehyde (*m/z* 45), acetone (*m/z* 59), isoprene (*m/z* 69), MEK (*m/z* 73) and the monoterpene α-pinene (*m/z* 81 and *m/z* 137) were present in the calibration gas standard, allowing sensitivities to be calculated directly. Due to reduced quadrupole transmission for high masses, monoterpenes were quantified using the fragment ion at *m/z* 81. For compounds not contained in the gas standard (acetic acid (*m/z* 61) and MVK and MACR (*m/z* 71)) empirical sensitivities were calculated. A relative transmission curve was created using the instrumental sensitivities calculated from the masses present in the standard, and from this curve sensitivities for the unknown masses were calculated (Davison et al., 2009; Taipale et al., 2008). Error in calibration using the gas standard was assumed to be below 15 %, whereas relative errors in calibrations using the relative transmission approach are < 30 % (Taipale et al., 2008).

2.2.2 PTR-ToF-MS calibration

Background measurements of the PTR-ToF-MS were made up to three times a day using zero air generated by a custom made catalytic converter. Calibrations were made using a calibration gas (Appel Riemer Environmental Inc., USA) which contained 16 compounds, with masses ranging from 33 to 180 amu. For VOCs not included in the calibration standard, the average instrument sensitivities towards the known C_xH_y, $C_xH_yO_z$ or $C_xH_yN_z$ compound families were used.

2.3 Calculation of volume mixing ratios

Mixing ratios by volume were calculated from data generated using the PTR-MS using a program written in LabVIEW (National Instruments, Austin, Texas, USA). Mixing ratios by volume (χ_{VOC}) were calculated from the raw PTR-MS data (in counts per second (cps)) using a method based on those of Taipale et al. (2008) and Tani et al. (2004).

$$\chi_{voc} = \frac{I(RH^+)_{norm}}{S_{norm}} \qquad (1)$$

where S_{norm} is the normalised sensitivity and $I(RH^+)_{norm}$ represents the background corrected normalised count rate (ncps) for the protonated compound R which was calculated as shown below.

$$I(RH^+)_{norm} = I(RH^+)\left(\frac{I_{norm}}{I(H_3O^+)+I(H_3O^+H_2O)}\right)\left(\frac{p_{norm}}{p_{drift}}\right)$$

$$-\frac{1}{n}\sum_{i=1}^{n} I(RH^+)_{zero,i}\left(\frac{I_{norm}}{I(H_3O^+)_{zero,i}+I(H_3O^+H_2O)_{zero,i}}\right)\left(\frac{p_{norm}}{p_{drift,zero,i}}\right) \quad (2)$$

where $I(RH^+)$, $I(H_3O^+)$ and $I(H_3O^+H_2O)$ represent the observed count rate for the protonated compound R, H_3O^+ and the $H_3O^+H_2O$ cluster, respectively. Subscript zero refers to zero air measurements, n is the number of zero air measurement cycles and p_{drift} is the drift tube pressure. The drift tube pressure was normalised to 2 mbar (p_{norm}) and the sum of the primary ion and first water cluster was normalised to a count rate of 10^6 cps (I_{norm}). The compound specific limit of detection (LoD) was calculated using the method described by Karl et al. (2003):

$$LoD = 2 \times \frac{\sigma_{Background}}{S_{VOC}} \quad (3)$$

where S_{VOC} is the instrumental sensitivity to the VOC and $\sigma_{Background}$ is the mean background normalised count rate.

2.4 Flux calculations from PTR-MS

The 25 min PTR-MS flux files were inspected and incomplete or disrupted files were removed. BVOC fluxes were then calculated using a program also written in LabVIEW, based upon the virtual disjunct eddy covariance technique (vDEC) developed by Karl et al. (2002), also termed continuous flow disjunct eddy covariance (Rinne et al., 2008). This method has been successfully applied in a number of studies (e.g. Davison et al., 2009; Langford et al., 2009; 2010a; 2010b; Misztal et al., 2011; Rinne et al. 2007). This approach allows direct calculation of fluxes of atmospheric constituents, as with standard eddy covariance, yet in this case sampling of scalar concentrations is not continuous. The flux, F_x, for each compound was calculated using a covariance function between the vertical wind velocity, w, and the VOC mixing ratios, χ:

$$F_x(\Delta t) = \frac{1}{N}\sum_{i=1}^{N} w'(i-\Delta t/\Delta t_w)\chi'(i) \quad (4)$$

where Δt is the lag time between the PTR-MS concentration measurements and the vertical wind velocity measurements from a sonic anemometer, Δt_w is the sampling interval between wind measurements (0.1 s), N is the number of PTR-MS measurement cycles in each 25 min averaging period (typically 306 in our study) and primes represent the momentary deviations from the mean concentration or vertical wind speed (e.g. $w = w' - \bar{w}$).

Variations in temperature, pressure and the performance of the sample line pump can cause small deviations in Δt. Therefore these values were calculated using a cross correlation function between w' and χ'. Lag times were calculated individually for each *m/z* monitored by the PTR-MS by selecting the absolute maximum value of the covariance function within a 30 s time window (MAX method, Taipale et al., 2010). This analysis resulted in a clear isoprene flux but for most masses a high proportion of the data fell below the limit of detection. These data, especially in the case of acetone, showed a significant amount of flux values with the opposite sign, "mirroring" the true flux. These "mirrored" points occur when the measured flux is of comparable magnitude to the total random error of the system (Langford et al., 2015). As the cross-correlation maximum is likely to be an over-estimate when the noise to signal ratio is greater than one, these points were substituted with fluxes calculated using a fixed lag time.

A histogram of isoprene lag times calculated using the MAX method is displayed in the Supplementary Information showing a clear maximum at 7.5 s. Therefore 7.5 s was chosen as the isoprene fixed lag time and fixed lag times for the other masses were calculated from the isoprene fixed lag time, accounting for the dwell times of the different compounds in the measurement cycle.

2.4.1 Flux quality assessment and potential losses

In order to assess the quality of each 25 min flux file, the resultant fluxes were subjected to three quality checks following a two-dimensional coordinate rotation which was applied to correct for tilting of the sonic anemometer (see Table S1 in the Supplementary Information document for summary). Following the criteria of Langford et al. (2010a), data points were labelled if the mean friction velocity (u_*) over the 25 min averaging period was found to be below 0.15 m s^{-1}. Data falling below this threshold predominantly occurred at night when wind velocity reached a minimum. Detection limits for each 25 min flux file were calculated using a method based on that of Wienhold et al. (1994) as applied by Spirig et al. (2005) where the signal of the flux at the true lag is compared to the background noise of the covariance function. The 95th percentile of the covariance function in the lag range 150-180 s was calculated and flux files falling below this value were labelled as having fallen below the LoD. Finally data points underwent a stationarity test as described by Foken and Wichura (1996), which assessed that stability of the flux across the 25 min averaging period, data points found to be generated from periods of non-stationarity were also labelled. Flux files in which all three tests were passed and where only the LoD test was failed were included in all further analysis. Files which failed the LoD test were included to prevent a positive bias being introduced to results. Flux files failing the stationarity check or falling below the u_* threshold were excluded from further analysis.

The integral turbulence characteristics were assessed using the FLUXNET criteria described by Foken et al. (2004). The turbulence at the Bosco Fontana field site was well developed with 87% of the data in the first three categories, defined by Foken et al. (2004) as suitable for fundamental research. Less than 1% of the data fell into category 9, characterised as data to be excluded under all circumstances.

The flux losses in the virtual disjunct eddy covariance system were assessed. Loss of flux at frequencies higher than the PTR-MS response time and/or dwell time was corrected for using the method described by Horst (1997). Correction factors in the range 1.01 - 1.23 were calculated and applied to each 25 min flux file with a mean correction of 8.8 %. Rotating the coordinates in order to set the vertical mean vertical wind velocity to 0 for each twenty five minute flux averaging period and block averaging itself act as a high pass flux filter (Moncrieff et al., 2004), leading to the loss of low frequency fluxes. The loss of these low frequency fluxes due to an insufficient averaging period is assessed in the Supplementary Information. Sensible heat flux data were averaged over 50, 75, 100 and 125 minutes before a coordinate rotation was applied and plotted against the sum of two, three, four and five 25 minute coordinate rotated flux files, respectively. The gradient of the fitted line between the two fluxes gives an estimate of the flux lost by the use of twenty five minute averaging periods. As is shown in Fig. S2 of the Supplementary Information, eddies with a time period between 25 and 125 minutes carry only an additional 2.8 % of the sensible heat flux. Therefore if we assume that the frequency of VOC and sensible heat fluxes are comparable, 1.0-3.6 % of the VOC flux is lost by limiting the averaging period to 25 minutes. This correction has not been applied to the displayed data as it is so small. The percentage of flux files in which > 25 % of the flux was found to be coming from outside the forest area was also assessed and found to be 26 %.

2.5 Flux calculations from PTR-ToF-MS

BVOC fluxes were calculated from PTR-ToF-MS data using the eddy covariance (EC) method similar to that described above for the PTR-MS. The PTR-ToF-MS flux analysis differed in that the cross correlation between w' and χ' was calculated using the method described by Park et al. (2013). Whilst in the PTR-MS measurement, the target compounds are predetermined through the measurement cycle, in the PTR-ToF-MS the entire high resolution mass spectrum can be used to search for compounds that carry a flux. PTR-ToF-MS data were analysed using the TOF Analyzer V2.45 as described by Müller et al. (2013) and TofTools (Junninen et al., 2010). An automated flux identification routine was then used to calculate the average of the absolute cross covariance functions during a mid-day period. The maximum value was then automatically selected from the averaged spectrum and checked against the manually selected noise level (10 σ_{noise}) to determine whether a flux was present.

The fluxes were filtered using the 70% stationary criteria as presented by Foken and Wichura (1996), as was applied to the PTR-MS data and corrected for loss of high frequency flux Horst (1997). For a more detailed description of the flux calculation from the PTR-ToF-MS see Schallhart et al. (2015).

2.6 Leaf level GC-MS measurements

A portable gas exchange system equipped with a controlled-environment 6-cm^2 broadleaf cuvette (LI6400, Li-COR, Lincoln, USA) was used to measure net photosynthetic rate (*A*) and stomatal conductance (g_s) at basal conditions of PAR (1000 µmol m^{-2} s^{-1}), leaf temperature (30 °C) and a CO_2 concentration (400 ppm) from fully expanded leaves. BVOC emission was recorded at basal conditions to ensure that steady state fluxes could be obtained and to enable comparison between different individual measurements. When *A* reached a steady-state, the outlet tube from the leaf cuvette was replaced with a Teflon tube, and the air stream exiting from the cuvette was used to sample BVOCs (according to the methodology in Loreto et al., 2001) by adsorbing them on to a silco-steel cartridge packed with 200 mg of tenax (Supelco, PA, USA). Tenax is a very hydrophobic and adsorbent material with high thermal stability generally used for trapping BVOC (Dettmer and Engewald, 2002). The flow rate through the leaf cuvette was maintained at 500 µmol s^{-1}, and a subsample of 200 mL min^{-}

^{1} (130 µmol s^{-1}) was pumped through the cartridge with an external pump (AP Buck pump VSS-1) for a total volume of 6 L of air. Blank samples of air without a leaf in the cuvette were collected every day before and after the BVOC samplings. Finally the cartridges were sealed and stored at 4 °C until analysis.

The cartridges were analyzed using a Perkin Elmer Clarus 580 gas-chromatograph coupled with a Clarus 560 Mass-Detector and a thermal-desorber Turbo Matrix (Perkin Elmer Inc., Waltham, MA, USA). The gas-chromatograph was equipped with an Elite-5-MS capillary column (30 m length, 250 µm diameter and 0.25 µm film thicknesses). The carrier gas was helium. The column oven temperature was kept at 40 °C for 5 min, then increased with a 5 °C min^{-1} ramp to 250 °C and maintained at 250 °C for 5 min. BVOC were identified using the NIST library provided with the GC/MS Turbomass software. GC peak retention time was substantiated by analysis of parent ions and main fragments of the spectra. Commercially available reference standards (gaseous standards, Rivoira, Milan, Italy and liquid standards, Sigma Aldrich, Milan, Italy) were used to create the calibration curves and to quantify the emissions. To normalize the BVOC results, the quantities of terpenes collected from the empty cuvette (blanks) were subtracted from the plant emission results.

2.7 Mapping tree species distribution

Tree species distribution data were obtained from Dalponte et al. (2007) who used a combination of Light Detection and Ranging (LIDAR) and hyperspectral data to develop a high resolution tree species distribution map of the Bosco Fontana natural reserve.

The overall accuracy (kappa coefficient) of this species map is particularly high (0.89), considering the number of classes (23) and the number of training samples (20% of the data are used in the training set and 80% in the test set) per class. The LIDAR channels provide relatively sparse information for discriminating between tree species, increasing the overall accuracy of the tree species assignment using the hyperspectral data by only 1 % but the LIDAR data significantly increase the accuracy of understory and underrepresented classes. The kappa coefficient of the main species is also very high (0.88-0.93) showing the effectiveness of this approach for species classification in a very complex forest with 20 different broad-leaves species, some of which, such as *Q. cerris*, *Q. robur* and *Q. rubra*, belong to same genus. For a more detailed discussion of the mapping results and methodology see Dalponte et al. (2007) and Dalponte et al. (2008).

3 Results and discussion

3.1 Meteorological conditions

The measurement campaign at Bosco Fontana ran from 01/06/2012 to 11/07/2012 (41 days) with data recorded using the PTR-MS from the 13/06/2012 to the 11/07/2012. The meteorological conditions recorded at the measurement site during this period are summarised in Fig. 1, times are reported in central European time (UTC + 1) as used throughout this paper. The campaign average flux footprint is displayed in Fig. 2. With the exception of two heavy thunderstorms, the first in the first week of June before measurements began and the second overnight on 6th July, there was no precipitation during the measurement period. During the measurement period ambient temperature varied from a low of 14 °C to a high of 35 °C with temperatures lowest early in the campaign. Daily photosynthetically active radiation (PAR) peaked within the range 1890-2105 μmol m^{-2} s^{-1} and the relative humidity during the campaign varied between 29 and 90 %. Winds were generally easterly or north westerly. For most of the campaign wind speeds were below 3.5 m s^{-1} but peaked at 5.6 m s^{-1} on 23rd June, with the mean wind speed for the campaign period of 1.6 m s^{-1}.

3.2 BVOC mixing ratios and fluxes

BVOC fluxes were recorded at the Bosco Fontana site using both the PTR-MS and the PTR-ToF-MS. Unless stated, the results displayed here were calculated from measurements made using the PTR-MS. Data analysis was carried out with the aid of the R openair package (Carslaw and Ropkins, 2012; R Core Team 2012). For a full discussion of all fluxes and concentrations recorded using the PTR-ToF-MS see Schallhart et al. (2015).

The mixing ratios of the eight BVOC species measured in flux mode using the PTR-MS are displayed in Fig. 3 and are summarised in Table 2 (for further details, see Fig. S6 of the Supplementary Information). These mixing ratios were calculated using the high frequency flux measurements so the presented mixing ratios are an average over 25 minutes. The mixing ratio LoDs, calculated as described above (Karl et al., 2003; Langford et al., 2009; Misztal et al., 2011) were in the same range as those calculated on previous campaigns (Langford et al., 2009; Misztal et al., 2011) and, with the exception of isoprene where the mixing ratio dropped towards zero at night, the recorded mixing ratios generally remained above their respective LoD.

Table 3 summarizes the flux data recorded during the Bosco Fontana measurement campaign. Wind speeds decreased at night, leading to a large proportion of the night time data falling below the u_* threshold of 0.15 m s^{-1}. Consequently, average emission fluxes of all eight compounds are reported for the daytime period 10:00-15:00 LT as well as for the whole campaign. Large fluxes of *m/z* 69 and *m/z* 81 (assigned to isoprene and monoterpenes respectively) were observed and are shown in Fig. 4. Fluxes of *m/z* 33, 45, 59, 61, 71 and 73 (assigned to methanol, acetaldehyde, acetone, acetic acid, MVK + MACR and MEK, respectively) were also observed, but these fluxes were weaker, leading to a high percentage of fluxes failing the LoD check. However, as is described by Langford et al. (2015), when these flux data are averaged to show the average diurnal cycle, it is appropriate to use a combined LoD value appropriate for the same period rather than the LoD attached specifically to each 25 min flux file. It is, though, essential that each individual flux period be processed carefully to avoid the introduction of a bias due to the use of the MAX method of time-lag identification. The LoD for the mean ($\overline{LoD}$) decreases with the square root of the number of samples averaged (N).

$$\overline{LoD} = \frac{1}{N}\sqrt{\sum_{i=1}^{N} LoD^2} \qquad (5)$$

Therefore, while the flux time series of methanol, acetaldehyde, acetone, acetic acid, MVK + MACR and MEK are not presented here, the campaign average diurnal fluxes are shown (Fig. 5). As discussed above, 25 min averaged flux files flagged as below the LoD were included in these diurnal averages. Flux files falling below the 0.15 m s^{-1} wind speed threshold were also included to prevent the night time flux being biased high for depositing compounds. For compounds showing emission, night-time fluxes are close to zero anyway and the application has little influence on the results. Data flagged for non-stationarity were excluded. For a more detailed discussion of the fluxes and mixing ratios of each BVOC and comparison made with other temperate and Mediterranean ecosystems, see the Supplementary Information.

The fluxes of isoprene and monoterpenes calculated using both the PTR-MS and the PTR-ToF-MS instruments are displayed in Fig. 4 and summarised in Table 3. The isoprene fluxes calculated using both instruments show very good correlation (R^2 = 0.91, slope 1.3 and intercept 0.17 mg m^{-2} h^{-1}). The monoterpene fluxes, calculated using *m/z* 81 with the PTR-MS and *m/z* 81.070 with the PTR-ToF-MS show an R^2 = 0.50. Three additional mass spectral peaks are observed at *m/z* 81 in the PTR-ToF-MS: *m/z* 80.92, 80.99 and 81.03, however statistically significant fluxes from these peaks could not be calculated using the PTR-ToF-MS. Owing to the lower sensitivity of the PTR-MS at *m/z* 81 and the lower sampling frequency of the disjunct sampling protocol (Rinne and Ammann 2012), the monoterpene flux calculated using this instrument is significantly noisier than the flux calculated using the PTR-ToF-MS.

PTR-MS and PTR-ToF-MS mass scans were averaged over a ten day period (14th – 24th June). A comparison of these mass scans over the range *m/z* 33 to 100 at unit mass resolution is displayed in Fig. 6, with masses reported relative to *m/z* 59 (acetone). A good agreement between the PTR-MS and PTR-ToF-MS is seen for all masses, except for *m/z* 33 where the PTR-MS gives a significantly higher signal. As both instruments have comparable sensitivities at this mass (11.6 and ca. 10-12 ncps $ppbv^{-1}$ for the PTR-MS and PTR-ToF-MS respectively) this discrepancy must be the result of interference from another ion at this mass. $O^{17}O^+$ could interfere with the methanol signal at *m/z* 33 but as a significant peak is not observed at *m/z* 34 ($O^{18}O^+$) a large contribution from $O^{17}O^+$ to m/z 33 is unlikely. This suggests that there is a greater formation of O_2H^+ in the PTR-MS than in the PTR-ToF-MS under these particular operation parameters. No major mass spectral peaks are observed in one instrument alone, indicating that there is no artefact formation or unexpected loss of chemical species with either instrument. The mass scans show a much cleaner spectrum than was reported by Misztal et al. (2011) above an oil palm plantation in South-East Asia, suggesting an atmosphere dominated by fewer chemical species at higher concentrations.

3.2.1 BVOC correlations

Scatter plots were used to investigate the relationship between the measured species. Methanol, acetone and MEK (Fig. 7) all showed a shift in the regression of the BVOCs with increasing temperature with two linear groupings observed, one at lower temperature (ca. < 20°C) and another at higher temperatures (ca. > 20°C). The change in regression could be a result of either by different proportions of BVOCs present in high and low temperature air masses or by two different sources contributing to the mixing ratios (most likely an atmospheric background and a photochemical source at higher temperatures). It is possible that a second compound could contribute to the nominal mass at higher temperatures but as few compounds have been reported to contribute to *m/z* 33 or 59, this seems unlikely.

3.2.2 Short-chain oxygenated BVOCs

A mean methanol mixing ratio of 6.2 ppbv at 4 m above the canopy was recorded over the duration of the campaign, making it the dominant BVOC observed at Bosco Fontana. Mean acetaldehyde, acetone and acetic acid mixing ratios were 3.4, 3.2 and 1.9 ppbv at 4 m above the canopy, respectively. Methanol, acetaldehyde and acetic acid mixing ratios all followed similar diurnal cycles (Fig. 3), with mixing ratios remaining stable through the night before a drop in the morning, probably caused by expansion of the planetary boundary layer after sunrise. Then mixing ratios increased again in the late afternoon as emissions accumulated in a shrinking boundary layer. Acetone mixing ratios remained on average stable throughout the day (Fig. 3). This would suggest a day-time source of acetone offsetting the dilution caused by expansion of the planetary boundary layer. As the flux of acetone, where observed, was very small this source must either be photochemical or transport from outside the forest.

The flux of methanol peaked at 0.49 mg m^{-2} h^{-1} with a mean day-time flux of 0.03 mg m^{-2} h^{-1} (Fig. 5). Methanol deposition was observed during the night and mornings followed by a rapid increase in methanol emission in the late morning and peaking in the early afternoon. Bidirectional exchanges of methanol have been reported previously (for example Fares et al., 2012; Karl et al., 2004) with methanol absorption/desorption thought to occur in thin water films within the canopy (Wohlfahrt et al., 2015). The mean morning (06:30-10:30 LT) methanol deposition velocity (V_d) at the measurement height (z_m) was calculated using the relationship (Misztal et al., 2011):

$$V_{\mathrm{d}}(z_m) = -\frac{F}{\chi(z_{\mathrm{m}})} \tag{6}$$

and was found to be 0.31 cm s^{-1}. The night-time deposition velocity was lower, 0.02 cm s^{-1}, falling at the bottom end of the 0.02 – 1.0 cm s^{-1} range reported by Wohlfahrt et al. (2015) from a review of eight different north hemisphere sites.

Acetic acid deposition was also observed in the morning, but any emission flux in the afternoon remained below the limit of detection, even if aggregated into mean diurnal cycles. The mean diurnal acetaldehyde flux is shown in Fig. 5. The flux increased from below the detection limit in late morning to a peak in the early afternoon before dropping again towards zero at night. The flux peaked at 0.44 mg m^{-2} h^{-1} on 29th June and the campaign mean day-time flux was 0.06 mg m^{-2} h^{-1}. As can be seen in Fig. 5, the acetone flux remained below the limit of detection for most of the day with a small positive flux observed in the late afternoon.

3.2.3 MVK + MACR and MEK

MVK and MACR are the main products formed following the first stage of isoprene oxidation in the atmosphere (Atkinson and Arey 2003), accounting for ca. 80% of the carbon. MACR can also be directly produced within plants as a by-product in the production of cyanogenic glycosides (Fall 2003) and experimental observation demonstrated that emissions of MVK and MACR increase with temperature stress (Jardine et al., 2012). The mid-day (10:00-15:00 LT) mixing ratios of MVK + MACR at 4 m above the canopy showed a positive correlation with those of isoprene (R^2 = 0.49), suggesting that the oxidation of isoprene was responsible for the formation of MVK and MACR.

The production of MVK and MACR from isoprene at the Bosco Fontana site has been modelled by Schallhart et al. (2015), who estimated that 4 - 27 % of the MVK + MACR flux was formed from isoprene oxidisation products. MVK and MACR mixing ratios recorded at 4 m above the canopy (Fig. 3) increase in the morning as isoprene concentrations rise, before boundary layer expansion causes them to drop in the middle of the day. The mixing ratios then increase again in the evening as the boundary layer contracts. The flux of MVK + MACR (Fig. 5) peaked in the early afternoon with a mean day-time flux of 0.05 mg m^{-2} h^{-1}. This flux is comparable to the 0.03 and 0.08 mg m^{-2} h^{-1} observed, respectively, by Kalogridis et al. (2014) and Spirig et al. (2005) over European oak and mixed forests.

MEK may be directly emitted by plants (Fall, 2003) or formed photochemically (Luecken et al., 2012). MEK mixing ratios 4 m above the forest canopy remained stable through the night at ca. 0.6 ppbv before dropping in the morning, probably caused by expansion of the planetary boundary layer, to ca. 0.3 ppbv and rising again in the evening (Fig. 3). A plot of the mixing ratios of MEK against those of acetone reveals a bimodal distribution suggesting two distinct sinks or sources (Fig. 7), the first occurring at lower temperatures (ca. 12-20 °C) with a MEK to acetone ratio of ca. 0.17 and the second at higher temperatures (ca. 20-34 °C) with a MEK to acetone ratio of ca. 0.06. A relationship between acetone and MEK has been reported by Riemer et al. (1998) who observed an MEK to acetone ratio of 0.07 at temperatures between 20 and 37 °C. This compares well with the observations at Bosco Fontana. This trend was not observed when data were coloured by PAR indicating that the bimodal distribution is not driven by the faster rate of reaction of MEK than of acetone with OH. A low MEK emission flux was observed in the afternoon with a mean day-time flux of 0.02 mg m^{-2} h^{-1}.

3.2.4 Isoprene and monoterpenes

Isoprene mixing ratios 4 m above the canopy began to rise in the mid-morning from a night-time zero, peaking in the late afternoon at ca. 2 ppbv before falling again to zero in the late evening (Fig. 3). Isoprene fluxes were not observed at night, but increased in the morning to a peak in the mid afternoon before dropping to zero again in the evening (Fig. 5) with a mean day-time flux of 1.9 mg m^{-2} h^{-1}.

Isoprene fluxes correlated with leaf temperature (estimated using a method based on that described by Nemitz et al. (2009) and explained in more detail in the Supplementary Information, R^2 = 0.73 for an exponential fit), PAR (R^2 = 0.75 for an exponential fit) and with sensible heat flux (H) (R^2 = 0.67). The relationship between isoprene fluxes and mixing ratios, temperature and PAR is displayed in Fig. 8. Table 4 compares isoprene flux measurements with the fluxes recorded during other field campaigns in the Mediterranean region and the isoprene emission factor under basal conditions. As would be expected, the flux of isoprene is shown to be highly dependent on ecosystem type. The fluxes observed on this campaign, when normalised to standard conditions, are lower than those observed over woodland dominated by isoprene emitting oak species due to the lower proportion of isoprene emitting species in the canopy but closer in magnitude to that observed over a mixed pine and oak forest.

The campaign mean monoterpene mixing ratio 4 m above the canopy was 0.2 ppbv. The diurnal profile (Fig. 3) shows a night-time mixing ratio of ca. 0.18 ppbv which increases to ca. 0.21 ppbv in the morning remaining stable through the day and dropping again to ca. 0.18 ppbv at night. The monoterpene flux (Fig. 5) peaked in the early afternoon with a campaign mean mid-day flux of 0.12 mg m^{-2} h^{-1}. Monoterpene mixing ratios were not significantly correlated with leaf surface temperature or with PAR (R^2 = 0.11 and 0.12 respectively). However, the flux displayed a correlation with both leaf surface temperature and PAR (R^2 = 0.44 and 0.39 respectively).

3.3 Calculation of isoprene and monoterpene canopy level emission factors

Although other approaches do exist, isoprene fluxes are widely modelled using the Model of Emissions of Gases and Aerosols from Nature (MEGAN, Guenther et al., 2006). MEGAN calculates isoprene fluxes based on the product of an emission activity factor (γ), a canopy loss and production factor (ρ) and a canopy emission factor (ε). Therefore, plotting isoprene flux against $\gamma \times \rho$ enables the calculation of a canopy-specific isoprene emission factor (Fig. 9), giving value of 1.68 mg m^{-2} h^{-1} at standard conditions (1000 µmol m^{-2} s^{-1} PAR and 303 K) for the campaign period. For the purpose of this work, ρ was assumed to be 0.96 and γ was calculated using the algorithms described by Guenther et al. (2006). Radiative transfer through the canopy was modelled using the model applied by Müller et al. (2008). This model was based on that of Goudriaan and van Laar (1994) and ambient temperature was recorded 4 m above the canopy. The standard light and temperature conditions for MEGAN canopy scale emissions factors are ~1500 µmol m^{-2} s^{-1} and 303 K (Guenther et al., 2006). In order to enable direct comparison between the GC-MS data and literature emissions factors, the factor which sets the emission activity to unity at standard conditions (C_{CE}) was increased to 1.42. This gave standard light and temperature conditions of 1000 µmol m^{-2} s^{-1} and 303 K, respectively.

The emission factor is lower than those calculated by Kalogridis et al. (2014) and Baghi et al. (2012) from oak (*Quercus pubescens*) dominated forests in southern France (7.4 and 5.4 mg m^{-2} h^{-1}, respectively). However, this is to be expected, owing to the high proportion of low or non-isoprene emitting species such as *Carpinus betulus, Corylus avellana, Sambucus nigra* and *Acer campestre* present in the forest at Bosco Fontana.

Monoterpene emission from plants may take the form of pool or *de novo* emission. Emission from stored pools is temperature controlled whereas *de novo* is driven by photosynthesis and is therefore controlled by light as well as temperature (Ghirardo et al., 2010). Emission from stored pools was modelled using the monoterpene-temperature relationship described by Guenther et al. (1995), this model correlated well with the observed monoterpene flux (PTR-ToF-MS) giving R^2 value of 0.55. In order to assess the effect of light on monoterpene emission, the residual values from the temperature only model were plotted against PAR (Fig. 10). The residuals displayed a correlation with PAR ($R^2 = 0.45$) indicating that light as well as temperature has a significant impact on monoterpene emissions from the forest canopy and therefore a significant proportion of monoterpene emission is *de novo* emission. However, in order to accurately assess the contribution of pool and *de novo* emissions to the canopy scale monoterpene flux, a species specific leaf level investigation would be required. A monoterpene canopy emission factor calculated using the MEGAN algorithms, which only simulate *de novo* emission, was found to be 0.14 mg m^{-2} h^{-1}.

3.4 Speciated bottom-up isoprene and monoterpene flux estimates derived from leaf-level measurements

Tree species distribution data combined with information on leaf-level isoprene and monoterpene emission rates and meteorological data were used to produce a “bottom-up” estimate of the total canopy level flux. Tree species distribution data were obtained from Dalponte et al. (2007), this tree species distribution map reveals an uneven distribution of isoprene emitting species within the forest canopy, with the two main isoprene emitting species (*Q. robur* and *Q. rubra*) concentrated in the south of the forest.

Leaf-level isoprene and monoterpene emissions from the dominant tree species were recorded using GC-MS (Table 5). Together these species represent 76.6 % of the total vegetation cover. Isoprene emission was dominated by *Q. robur* and *Q. rubra* with *C. avellana* and *C. betulus* the highest monoterpene emitting species. The isoprene emission recorded for both oak species was lower than that previously reported (Karl et al., 2009; Keenan et al., 2009). For species where GC-MS data were not available, literature values were used. Leaf-level emission factors for minor species for which no GC-MS measurements were made were taken from Karl et al. (2009) with the exception *Rubus* sp. (Owen et al., 2001) and *Acer negundo* and *Morus* sp. (Benjamin et al., 1996). Emission factors taken from the literature were converted from µg g_{DW}^{-1} h^{-1} to mg m^{-2} h^{-1} using the mean leaf mass to area ratio, 115 g_{DW} m^{-2}, reported by Niinemets (1999) from a study of ca. 600 species. The leaf-level emissions data were then scaled up to a canopy level using the MEGAN algorithms (Guenther et al., 2006) and incorporated measured PAR and temperature values averaged over 30 minutes and a single sided leaf area index (LAI, m^2/m^2) of 5.5.

The hyperspectral/LIDAR data of Dalponte et al. (2007) was remapped onto a grid centred on the measurement site, with a resolution of 5 m^2, providing fractional ground cover by each of the 20 tree species within each grid cell. The contribution of each grid cell to each 25-minute flux measurement was then calculated at 5 m^2 resolution using a high resolution 2-D footprint model based on Kormann and Meixner (2001) similar to that described by Neftel et al. (2008). Finally, the MEGAN algorithm was applied to all plant species using the 25-minute meteorology. The information was combined to provide a bottom-up estimate of the flux that the canopy-scale measurements should have detected, based on the leaf-level data. This footprint and species dependent bottom-up flux estimate showed significantly better agreement with the measured isoprene flux (R^2 = 0.75, slope = 0.56) than was observed when the canopy-scale isoprene emission factor calculated above was used (R^2 = 0.65, slope = 0.76). This demonstrates the large effect an uneven distribution of isoprene sources can have on the above canopy flux, even within what appears to be a uniform canopy, and the benefit for accounting for spatial species distributions in uniform vegetation canopies.

However, despite capturing the shape of the flux time series, the bottom-up flux underestimated the magnitude of the flux, capturing 56 % of the isoprene flux as measured by vDEC. This could in part be caused by changes in vegetation cover between the tree distribution mapping in 2008 and the flux measurements in 2012. There are anecdotal reports that *Populus* sp. coverage has increased in the understory vegetation but it is unlikely that, despite their high rates of growth, the *Populus* coverage changed significantly in the 4 years between mapping and this campaign. Since 2008, the non-native *Q. rubra* is gradually being removed from the forest. However, this does not explain the discrepancy between the vDEC isoprene flux measurements and the bottom-up flux estimate as the reduction in the number of *Q. rubra* trees should have decreased the flux. Whilst the hyperspectral/LIDAR tree species data for this site provides a unique opportunity for comparing the canopy-scale measurements with a detailed bottom-up estimate, the hyperspectral/LIDAR data only provides information on projected tree species area as seen from above, whilst the flux is regulated by leaf mass and its exposure to radiation. Thus there are uncertainties in the ability of the hyperspectral/LIDAR to detect understorey vegetation and a single conversion factor was used between projected tree area and leaf mass. However, understorey vegetation is less exposed to sunlight reducing its emission. Indeed, the main reason for the underestimate of isoprene flux is probably that the leaf level isoprene emission rate recorded from the leaves sampled at ground level (albeit taken at the edge of sun exposed clearings) are not representative of those at the canopy top. Substituting the measured *Q. robur* and *Q. rubra* emission factors with those reported by Karl et al. (2009) caused the bottom-up estimate to give 130 % of the measured flux and improved the correlation between bottom-up estimates and canopy-scale measurements further.

The speciated monoterpene flux (calculated using GC-MS data and literature values for species where GC-MS data was not available) also showed good agreement with the above canopy flux (R^2 = 0.72) and captured 57 % of the flux. The discrepancy between the magnitude of the speciated monoterpene flux and the above canopy flux could be partially explained by loss of monoterpenes through within canopy oxidation. Schallhart et al. (2015) investigated the flux loss due to chemical degradation using measured concentrations of ozone and NO_2 together with calculated OH and NO_3 concentrations. They found that 5-20 % of the monoterpene flux was lost via degradation (in comparison just 3-5 % of the isoprene flux was lost). The bottom-up monoterpene flux estimate may also have been affected by the changes to the tree species distribution in the 4 years between mapping and this campaign, as discussed above, and by deposition of monoterpenes within the forest canopy.

The contribution of different species to the isoprene and monoterpene fluxes over the course of an example day is shown in Fig. 11. As is shown, the isoprene flux was dominated by *Q. robur* but was sensitive to the species composition within the flux footprint. The change in wind direction around 14:00 LT reduced the contribution of *Q. rubra* to the total flux, with the contribution of *Populus* × *canescens* increasing significantly. The monoterpene flux was predicted to have been dominated by *C. betulus*, the dominant tree species in the canopy at Bosco Fontana. A greater number of tree species contributed to the monoterpene flux, and emissions were therefore much more uniform across the canopy and less affected by changes in wind direction.

The fit between the above canopy measured isoprene and monoterpene fluxes and the “bottom-up” flux estimate was improved by optimising the leaf-level emission factors, within the constraints displayed in Table 6, using Chi^2 minimisation as implemented by the solver function in Microsoft Excel. Use of the optimised isoprene and monoterpene emission factors gave good correlations with measured fluxes (R^2 values of 0.75 and 0.76, respectively). The optimised isoprene and monoterpene emission factors are presented in Table 6 and show a reasonable agreement with literature values (Karl et al., 2009).

4 Conclusions

Direct above-canopy fluxes of methanol, acetaldehyde, acetic acid, isoprene, MVK + MACR, MEK and monoterpenes were calculated using the method of virtual disjunct eddy covariance from mixing ratio data obtained with a PTR-MS above a semi-natural mixed oak and hornbeam forest in northern Italy from June 13th to July 11th 2012. Isoprene was the dominant BVOC emitted with a mean day-time flux of 1.91 mg m^{-2} h^{-1}. When normalised to standard conditions (temperature of 30 °C, PAR of 1000 µmol m^{-2} s^{-1}) using the MEGAN model (Guenther et al., 2006), a canopy scale emission factor of 1.68 mg m^{-2} h^{-1} was derived. Mixing ratios of VOCs measured at 4 m above the forest canopy were dominated by those of methanol, with a campaign mean mixing ratio of 6.2 ppbv.

The isoprene fluxes obtained using the PTR-MS/vDEC system showed good agreement with those obtained using a direct eddy covariance (with mixing ratios by volume measured with a fast response PTR-ToF-MS instrument). Monoterpene fluxes recorded using the PTR-MS were noisier and marginally higher than those recorded using the PTR-ToF-MS due to a lower sensitivity and, probably, the inclusion of isobaric compounds. Comparison of mass scan data generated using the PTR-MS and PTR-ToF-MS (*m/z* 33-100) showed very good agreement with no significant masses observed in one instrument but not in the other.

Up-scaling leaf-level isoprene and monoterpene emissions to the canopy scale, using a high spatial resolution tree species database and a 2D footprint model, showed significantly better correlation with the measured above canopy fluxes than was obtained using a canopy scale emission factor. Leaf-level isoprene emissions resulted in an underestimate of the above-canopy isoprene flux and this was assumed to be the result of differences in isoprene emission rates from leaves sampled at ground-level and those at the canopy top.

Overall, the data obtained give confidence in the measurement of biogenic VOC fluxes by the method of virtual disjunct eddy covariance and highlight the importance of using leaf-level emissions data from sun-lit canopy-top leaves when up-scaling leaf-level emissions to produce a “bottom-up” canopy-scale emissions estimate.

Acknowledgements

W.J.F. Acton would like to thank Alex Guenther for his advice on the use of MEGAN. This work was funded by the EU FP7 grants ÉCLAIRE (grant 282910) and PEGASOS (grant 265148), as well as by a BBSRC/Ionicon Analytik GmbH Industrial CASE studentship awarded to W.J.F.A. We acknowledge access to the measurement site provided by the Italian Corpo forestale dello Stato and provision of the site infrastructure by the Catholic University of Italy at Brescia and in particular by Giacomo Gerosa, Angelo Finco and Riccardo Marzuoli.

References

Arneth A., Monson R.K., Schurgers G., Niinemets Ü. and Palmer P.I.: Why are estimates of global terrestrial isoprene emissions so similar (and why is this not so for monoterpenes)? Atmospheric Chemistry and Physics, 8, 4605-4620, 2008.

Ashmore M.R.: Assessing the future global impacts of ozone on vegetation. Plant, Cell and Environment, 28, pp.949–964, 2005.

Atkinson R. and Arey J.: Gas-phase tropospheric chemistry of biogenic volatile organic compounds: a review. Atmospheric Environment, 37, 197-219, 2003.

Baghi R., Durand P., Jambert C., Jarnot C., Delon C., Serça D., Striebig N., Ferlicoq M. and Keravec P.: A new disjunct eddy-covariance system for BVOC flux measurements –

validation on CO_2 and H_2O fluxes. Atmospheric Measurement Techniques, 5, 3119-3132, 2012.

Bigi A., Ghermandi G. and Harrison R.M.: Analysis of the air pollution climate at a background site in the Po valley. Journal of Environmental Monitoring, 14, 552-563, 2011.

Blake R.S., Monks P.S., and Ellis A.M.: Proton-Transfer Reaction Mass Spectrometry. Chemical Reviews, 109, 861-896, 2009.

Benjamin M.T., Sudol M., Bloch L. and Winer A.M.: Low-emitting urban forests: A taxonomic methodology for assigning isoprene and monoterpene emission rates. Atmospheric Environment, 30(9), 1437-1452, 1996.

Carslaw D. C. and Ropkins K.: openair — an R package for air quality data analysis. Environmental Modelling and Software, 27-28, 52-61, 2012.

Dalponte M., Gianelle D. and Bruzzone L.: Use of hyperspectral and LIDAR data for classification of complex forest areas, in: Canopy Analysis and Dynamics of a Floodplain Forest, Cierre Edizioni, Verona, Italy, 25–37, 2007

Dalponte M., Bruzzone L. and Gianelle D.: Fusion of hyperspectral and LIDAR remote sensing data for classification of complex forest areas. IEEE Transactions on Geoscience and Remote Sensing, 46(5), 1416-1427, 2008.

Davison B., Taipale R., Langford B., Misztal P., Fares S., Matteucci G., Loreto F., Cape J.N., Rinne J. and Hewitt C.N.: Concentrations and fluxes of biogenic volatile organic compounds above a Mediterranean macchia ecosystem in western Italy. Biogeosciences, 6, 1655-1670, 2009.

de Gouw J.A., Goldan P.D., Warneke C., Kuster W.C., Roberts J.M., Marchewka M., Bertman S.B., Pszenny A.A.P. and Keene W.C.: Validation of proton transfer reaction-mass spectrometry (PTR-MS) measurements of gas-phase organic compounds in the atmosphere during the New England Air Quality Study (NEAQS) in 2002. Journal of Geophysical Research, 108, D214682, doi:10.1029/2003JD003863, 2003.

de Gouw J. and Warneke C.: Measurements of volatile organic compounds in the earth's atmosphere using proton transfer-reaction mass spectrometry. Mass Spectrometry Reviews, 26, 223-257, 2007.

Decesari S., Allan J., Plass-Duelmer C., Williams B.J., Paglione M., Facchini M.C., O'Dowd C., Harrison R.M., Gietl J.K., Coe H., Giulianelli L., Gobbi G.P., Lanconelli C., Carbone C., Worsnop D., Lambe A.T., Ahern A.T., Moretti F., Tagliavini E., Elste T., Gilde S., Zhang Y. and Dall'Osto M.: Measurements of the aerosol chemical composition and mixing state in the Po Valley using multiple spectroscopic techniques. Atmospheric Chemistry and Physics, 14, 12109-12132, 2014.

Dettmer K., Engewald W.: Adsorbent materials commonly used in air analysis for adsorptive enrichment and thermal desorption of volatile organic compounds. Analytical Biochemistry 373, 490-500, 2002.

Fall R.: Abundant Oxygenates in the Atmosphere: A Biochemical Perspective. Chemical reviews, 103, 4941-4951, 2003.

Fares S., Park J.-H., Gentner D.R., Weber R., Ormeño E., Karlik J. and Goldstein A.H.: Seasonal cycles of biogenic volatile organic compound fluxes and concentrations in a California citrus orchard. Atmospheric Chemistry and Physics, 12, 9865–9880, 2012.

Fares S., Schnitzhofer R., Jiang X., Guenther A., Hansel A. and Loreto F.: Observations of diurnal to weekly variations of monoterpene-dominated fluxes of volatile organic compounds from mediterranean forests: implications for regional modeling. Environmental Science & Technology, 47, 11073-11082, 2013.

Fehsenfeld F., Calvert J., Fall R., Goldan P., Guenther A.B., Hewitt C.N., Lamb B., Liu S., Trainer M., Westberg H. and Zimmerman P.: Emissions of volatile organic compounds from vegetation and the implications for atmospheric chemistry. Global Biogeochemical Cycles, 6, 389–430, 1992.

Foken, T. and Wichura, B.: Tools for quality assessment of surface- based flux measurements. Agricultural and Forest Meteorology, 78, 83–105, 1996.

Foken T., Göckede M., Mauder M., Mahrt L., Amiro B., and Munger W.: Post-field data quality control, in: Handbook of Micrometeorology: A guide for surface flux measurement and analysis, edited by: Lee, W. M. X. and Law, B., Dordrecht, Kluer Academic Publishers, 29, 181–203, 2004.

Ghirardo A., Koch K., Taipale R., Zimmer I., Schnitzler J.-P. and Rinne J.: Determination of de novo and pool emissions of terpenes from four common boreal/alpine trees by $^{13}CO_2$ labelling and PTR-MS analysis. Plant, Cell and Environment, 33, 781-792, 2010.

Goudriaan, J. and van Laar, H.: Modelling Potential Crop Growth Processes. Textbook with Exercises. Kluwer Academic Publishers, Dordrecht, The Netherlands, 1994.

Graus, M., Müller, M. and Hansel, A.: High resolution PTR-TOF: Quantification and formula confirmation of VOC in real time. Journal of the American Society for Mass Spectrometry, 21, 1037-1044, 2010.

Guenther A., Hewitt C.N., Erickson D., Fall R., Geron C., Graedel T., Harley P., Klinger L., Lerdau M., McKay W.A., Pierce T., Scholes B., Steinbrecher R., Tallamraju R., Taylor J. and Zimmerman P.: A global model for natural volatile organic compound emissions. Journal of Geophysical Research, 100(D5), 8873–8892, 1995.

Guenther A., Karl T., Harley P., Wiedinmyer C., Palmer P.I. and Geron C.: Estimates of global terrestrial isoprene emissions using MEGAN (Model of Emissions of Gases and Aerosols from Nature). Atmospheric Chemistry and Physics, 6, 3180-3210, 2006.

Guenther, A. B., Jiang, X., Heald, C. L., Sakulyanontvittaya, T., Duhl, T., Emmons, L. K., and Wang, X.: The Model of Emissions of Gases and Aerosols from Nature version 2.1 (MEGAN2.1): an extended and updated framework for modeling biogenic emissions, Geoscientific Model Development, 5, 1471-1492, 2012.

Hallquist M., Wenger J.C., Baltensperger U., Rudich Y., Simpson D., Claeys M., Dommen J., Donahue N.M., George C., Goldstein A.H., Hamilton J.F., Herrmann H., Hoffmann T., Iinuma Y., Jang M., Jenkin M.E., Jimenez J.L., Kiendler-Scharr A., Maenhaut W., Mcfiggans G., Mentel T.F., Monod A., Prévot A.S.H., Seinfeld J.H., Surratt J.D., Szmigielski R. and Wildt J.: The formation, properties and impact of secondary organic aerosol: current and emerging issues. Atmospheric Chemistry and Physics, 9, 5155-5236, 2009.

Hansel A., Jordan A., Holzinger R., Prazeller P., Vogel W. and Lindinger W.: Proton transfer reaction mass spectrometry: on-line trace gas analysis at the ppb level. International Journal of Mass Spectrometry and Ion Processes, 149/150, 609-619, 1995.

Hayward S., Hewitt C.N., Sartin J.H. and Owen S.M.: Performance characteristics and applications of a proton transfer reaction-mass spectrometer for measuring volatile organic compounds in ambient air. Environmental Science & Technology, 36(7), 1554-1560, 2002.

Hewitt C.N., Hayward S. and Tani A.: The application of proton transfer reaction-mass spectrometry (PTR-MS) to the monitoring and analysis of volatile organic compounds in the atmosphere. Journal of Environmental Monitoring, 5, 1-7, 2003.

Jardine K.J., Monson R.K., Abrell L., Saleska S.R., Arneth, A., Jardine A., Ishida F.Y., Serrano A.M.Y., Artaxo P., Karl T., Fares S., Goldstein A., Loreto F. and Huxman, T.: Within-plant isoprene oxidation confirmed by direct emissions of oxidation products methyl vinyl ketone and methacrolein. Global Change Biology, 18, 973–984, 2012.

Jordan A., Haidacher S., Hanel G., Hartungen E., Märk L., Seehauser H., Schottkowsky R., Sulzer P., and Märk, T. D.: A high resolution and high sensitivity proton-transfer-reaction time-of-flight mass spectrometer (PTR-TOF-MS), International Journal of Mass Spectrometry, 286, 122–128, 2009.

Junninen H., Ehn M., Petäjä T., Luosujärvi L., Kotiaho T., Kostiainen R., Rohner U., Gonin M., Fuhrer K., Kulmala M. and Worsnop D.R.: A high-resolution mass spectrometer to measure atmospheric ion composition. Atmospheric Measurement Techniques, 3(4), 1039-1053, 2010.

Kalogridis C., Gros V., Sarda-Esteve R., Langford B., Loubet B., Bonsang B., Bonnaire N., Nemitz E., Genard A.-C., Boissard C., Fernandez C., Ormeño E., Baisnée D., Reiter I. and Lathière J.: Concentrations and fluxes of isoprene and oxygenated VOCs at a French Mediterranean oak forest. Atmospheric Chemistry and Physics, 14, 10085–10102, 2014.

Karl M., Guenther A., Köble R., Leip A. and Seufert G.: A new European plant-specific emission inventory of biogenic volatile organic compounds for use in atmospheric transport models. Biogeosciences, 6, 1059-1087, 2009.

Karl T.G., Spirig C., Rinne J., Stroud C., Prevost P., Greenberg J., Fall R. and Guenther A.: Virtual disjunct eddy covariance measurements of organic compound fluxes from a subalpine forest using proton transfer reaction mass spectrometry. Atmospheric Chemistry and Physics, 2, 279-291, 2002.

Karl T., Guenther A., Spirig C., Hansel A. and Fall R.: Seasonal variation of biogenic VOC emissions above a mixed hardwood forest in northern Michigan. Geophysical Research Letters, 30, 2186, doi:10.1029/2003GL018432, 2003.

Karl T., Potosnak M., Guenther A., Clark D., Walker J., Herrick J.D. and Geron C.: Exchange processes of volatile organic compounds above a tropical rain forest: Implications for modeling tropospheric chemistry above dense vegetation. Journal of Geophysical Research, 109, D18306, doi:10.1029/2004JD004738, 2004.

Keenan T., Niinemets Ü., Sabate S., Gracia C. and Peñuelas J.: Process based inventory of isoprenoid emissions from European forests: model comparisons, current knowledge and uncertainties. Atmospheric Chemistry and Physics, 9, 4053-4076, 2009.

Kormann R. and Meixner F. X.: An analytical footprint model for non-neutral stratification. Boundary-Layer Meteorology, 99, 207-224, 2001.

Langford B., Davison B., Nemitz B. and Hewitt C.N.: Mixing ratios and eddy covariance flux measurements of volatile organic compounds from an urban canopy (Manchester, UK). Atmospheric Chemistry and Physics, 9, 1971-1987, 2009.

Langford B., Misztal P.K., Nemitz E., Davison B., Helfter C., Pugh T.A.M., MacKenzie R.M., Lim S.F. and Hewitt C.N.: Fluxes and concentrations of volatile organic compounds from a South-East Asian tropical rainforest. Atmospheric Chemistry and Physics, 10, 8391-8412, 2010a.

Langford B., Nemitz E., House E., Philips G.J., Famulari D., Davison B., Hopkins J.R., Lewis A.C. and Hewitt C.N.: Fluxes and concentrations of volatile organic compounds above central London, UK. Atmospheric Chemistry and Physics, 10, 627-645, 2010b.

Langford B., Acton W., Ammann C., Valach A. and Nemitz E.: Eddy-covariance data with low signal-to-noise ratio: time-lag determination, uncertainties and limit of detection. Atmospheric Measurement Techniques Discussions, 8, 2913–2955, 2015.

Lindinger, W., Hansel, A. and Jordan, A.: Proton-transfer-reaction mass spectrometry (PTR-MS): On-line monitoring of volatile organic compounds at pptv levels. Chemical Society Reviews, 27, 347–354, 1998.

Loreto F., Fischbach R.J., Schnitzler J.P., Ciccioli P., Brancaleoni E., Calfapietra C., Seufert G.: Monoterpene emission and monoterpene synthase activities in the Mediterranean evergreen oak Quercus ilex L. grown at elevated CO2 concentrations. Global Change Biology, 7, 709-717, 2001.

Luecken D.J., Hutzell W.T., Strum M.L. and Pouliot G.A.: Regional sources of atmospheric formaldehyde and acetaldehyde, and implications for atmospheric modelling. Atmospheric Environment, 47, 477-490, 2012.

Misztal P.K., Nemitz E., Langford B., Di Marco C.F., Phillips G.J., Hewitt C.N., MacKenzie A.R., Owen S.M., Fowler D., Heal M.R. and Cape J.N.: Direct ecosystem fluxes of volatile organic compounds from oil palms in South-East Asia. Atmospheric Chemistry and Physics, 11, 8995-9017, 2011.

Monks P. S., Granier C., Fuzzi S., Stohl A., Williams M. L., Akimoto H., Amann M., Baklanov A., Baltensperger U., Bey I., Blake N., Blake R. S., Carslaw K., Cooper O. R., Dentener F., Fowler D., Fragkou E., Frost G. J., Generoso S., Ginoux P., Grewe V., Guenther

A., Hansson H. C., Henne S., Hjorth J., Hofzumahaus A., Huntrieser H., Isaksen I. S. A., Jenkin M. E., Kaiser J., Kanakidou M., Klimont Z., Kulmala M., Laj P., Lawrence M. G., Lee J. D., Liousse C., Maione M., Mcfiggans G., Metzger A., Mieville A., Moussiopoulos N., Orlando J. J., O'Dowd C. D., Palmer P. I., Parrish D. D., Petzold A., Platt U., Pöschl U., Prévôt A. S. H., Reeves C. E., Reimann S., Rudich Y., Sellegri K., Steinbrecher R., Simpson D., ten Brink H., Theloke J., van der Werf G. R., Vautard R., Vestreng V., Vlachokostas Ch. and von Glasow R.: Atmospheric composition change – global and regional air quality. Atmospheric Environment, 43, 5268–5350, doi:10.1016/j.atmosenv.2009.08.021, 2009.

Moncrieff J., Clement R., Finnigan J. and Meyers T.: Averaging, detrending, and filtering of eddy covariance time series, in: Handbook of Micrometeorology: A guide for surface flux measurement and analysis, edited by: Lee W.M.X. and Law B., Kluer Academic Publishers, Dordrecht, 2004.

Müller J.-F., Stavrakou, T., Wallens S., De Smedt I., Van Roozendael M., Potosnak, J., Rinne, J., Munger B., Goldstein, A. and Guenther A.B.: Global isoprene emissions estimated using MEGAN, ECMWF analyses and a detailed canopy environment model. Atmospheric Chemistry and Physics, 8, 1329-1341, 2008.

Müller M., Mikoviny T., Jud W., D'Anna B. and Wisthaler A. A new software tool for the analysis of high resolution PTR-TOF mass spectra. Chemometrics and Intelligent Laboratory Systems, 127, 158-165, 2013

Neftel A., Spirig C. and Ammann C.: Application and test of a simple tool for operational footprint evaluations. Environmental Pollution, 152, 644-652, 2008.

Nemitz E., Hargreaves K.J., Neftel A., Loubet B., Cellier P., Dorsey R.J., Flynn M., Hensen A., Weidinger T., Meszaros R., Horvath L., Dämmgen U., Frühauf C., Löpmeier F.J., Gallagher M.W. and Sutton M.A.: Intercomparison and assessment of turbulent and physiological exchange parameters of grassland. Biogeosciences, 6, 1445–1466, 2009.

Niinemets, Ü: Research review. Components of leaf dry mass per area – thickness and density – alter leaf photosynthetic capacity in reverse directions in woody plants. New Phytologist, 144, 35-47, 1999.

Owen S.M., Boissard C. and Hewitt C.N.: Volatile organic compounds (VOCs) emitted from 40 Mediterranean plant species: VOC speciation and extrapolation to habitat scale. Atmospheric Environment, 35, 5393-5409, 2001.

Park J.-H., Goldstein A.H., Timkovsky J., Fares S., Weber R., Karlik J., and Holzinger R.: Active atmosphere-ecosystem exchange of the vast majority of detected volatile organic compounds. Science, 341, 643-647, 2013.

R Core Team: R: A language and environment for statistical computing. R Foundation for Statistical Computing, Vienna, Austria. ISBN 3-900051-07-0, URL http://www.R-project.org/ (last access: 18 September 2015), 2012.

Riemer, D., Pos W., Milne P., Farmer C., Zika R., Apel E., Olszyna K., Kliendienst T. Lonneman W., Bertman S., Shepson P. and Starn T.: Observations of nonmethane hydrocarbons and oxygenated volatile organic compounds at a rural site. Journal of Geophysical Research, 103, 28111-28128, 1998.

Rinne J., Taipale R., Markkanen T., Ruuskanen T.M., Hellén H., Kajos M.K., Vesala T., and Kulmala M.: Hydrocarbon fluxes above a Scots pine forest canopy: measurements and modelling. Atmospheric Chemistry and Physics, 7, 3361–3372, 2007.

Rinne J., Douffet T., Prigent Y. and Durand P.: Field comparison of disjunct and conventional eddy covariance techniques for trace gas flux measurements. Environmental Pollution, 152, 630-635, 2008.

Rinne J. and Ammann C.: Disjunct Eddy Covariance Method, in: Eddy covariance: A practical guide to measurement and data, edited by: Aubinet M., Vesala T. and Papale D., Springer, New York, USA, 2012.

Rivera-Rios J.C., Nguyen T.B., Crounse J.D., Jud W., St. Clair J.M., Mikoviny T., Gilman J.B., Lerner B.M., Kaiser J.B., de Gouw J., Wisthaler A., Hansel A., Wennberg P.O., Seinfeld J.H. and Keutsch F.N.: Conversion of hydroperoxides to carbonyls in field and laboratory instrumentation: Observational bias in diagnosing pristine versus anthropogenically controlled atmospheric chemistry. Geophysical Research Letters, 41, 8645-8651, 2014.

Royal Society, Ground-level ozone in the 21st century: Future trends, impacts and policy implications: Science policy report 15/08. The Royal Society, London. 2008.

Schallhart S., Rantala P., Nemitz E., Mogensen D., Tillmann R., Mentel T.F., Rinne J. and Ruuskanen T.M.: Characterization of ecosystem scale VOC exchange at a Mediterranean oak-hornbeam forest, Atmospheric Chemistry and Physics Discussions, 15, 27627–27673, 2015.

Spirig C., Neftel A., Ammann C., Dommen J., Grabmer W., Thielmann A., Schaub A., Beauchamp J., Wistthaler A. and Hansel A.: Eddy covariance flux measurements of biogenic VOCs during ECHO 2003 using proton transfer reaction mass spectrometry. Atmospheric Chemistry and Physics, 5, 465-481, 2005.

Taipale R., Ruuskanen T.M., Rinne J., Kajos M.K., Hakola H., Pohja T. and Kulmala M.: Technical Note: Quantitative long-term measurements of VOC concentrations by PTR-MS – measurement, calibration, and volume mixing ratio calculation methods. Atmospheric Chemistry and Physics, 8, 6681-6698, 2008.

Taipale R., Ruuskanen T.M. and Rinne J.: Lag time determination in DEC measurements with PTR-MS. Atmospheric Measurement Techniques, 3, 853-862, 2010.

Tani A., Hayward S., Hansel A. and Hewitt C.N.: Effect of water vapour pressure on monoterpene measurements using proton transfer reaction-mass spectrometry (PTR-MS). International Journal of Mass Spectrometry, 239, 161-169, 2004.

Wienhold F.G., Frahm H. and Harris G.W.: Measurements of N_2O fluxes from fertilized grassland using a fast response tunable diode laser spectrometer. Journal of Geophysical Research, 99, 16557-16567, 1994.

Wohlfahrt G., Amelynck C., Ammann C., Arneth A., Bamberger I., Goldstein A.H., Gu L., Guenther A., Hansel A., Heinesch B., Holst T., Hörtnagl L., Karl T., Laffineur Q., Neftel A., McKinney K., Munger J.W., Pallardy S.G., Schade G.W., Seco R., Schoon N.: An ecosystem-scale perspective of the net land methanol flux: synthesis of micrometeorological flux measurements. Atmospheric Chemistry and Physics Discussions, 15, 2577-2613, 2015.

Table 1. Unit masses measured using the PTR-MS during the ÉCLAIRE campaign at Bosco Fontana and the exact masses observed using the PTR-ToF-MS. Where the PTR-MS sensitivity was calculated directly from a compound in the calibration standard this compound is indicated in brackets. At *m/z* 61 and 71 the sensitivity was calculated from a transmission curve.

Unit mass (PTR-MS)	Exact mass (PTR-ToF-MS)	Contributing compound(s)	Formula	PTR-MS sensitivity (ncps ppbv^{-1})
21	21.023	Water isotope	$H_3{}^{18}O^+$	-
33	32.997	Oxygen isotope	$O^{17}O^+$	11.60 (methanol)
	33.033	Methanol	CH_5O^+	
39	39.033	Water cluster	$H_5O^{18}O^+$	-
45	44.997	Protonated carbon dioxide	$C_1H_1O_2^+$	9.90 (acetaldehyde)
	45.033	Acetaldehyde	$C_2H_5O^+$	
59	59.049	Acetone	$C_3H_7O^+$	8.82 (acetone)
	59.049	Propanal	$C_3H_7O^+$	
61	61.028	Acetic acid	$C_2H_5O_2$	8.40 (transmission curve)
69	69.0699	Isoprene	$C_5H_9^+$	3.80 (isoprene)
	69.0699	2-Methyl-3-buten-2-ol fragment	$C_5H_9^+$	
	69.0699	Methyl butanal fragment	$C_5H_9^+$	
	69.0699		$C_5H_9^+$	
71	71.049	Methyl vinyl ketone	$C_4H_7O^+$	5.29 (transmission curve)
	71.049	Methacrolein	$C_4H_7O^+$	
	71.085	Unknown	$C_5H_{11}^+$	
73	73.026	Unknown	$C_3H_5O_2^+$	5.87 (Methyl ethyl ketone)
	73.047	Unknown	Unknown	
	73.065	Methyl ethyl ketone	$C_4H_9O^+$	
	73.065	Butanal	$C_4H_9O^+$	

81	80.997	Unknown	$C_4H_1O_2^+$	1.59 (α-pinene fragment)
	81.033	Unknown	$C_5H_5O^+$	
	81.070	Monoterpene fragment	$C_6H_9^+$	
	81.070	Hexenal fragment	$C_6H_9^+$	
137	137.056	Unknown	Unknown	0.16 (α-pinene)
	137.133	Monoterpenes	$C_{10}H_{17}^+$	

Table 2. Summary of the bVOC mixing ratios (ppbv) recorded at 4 m above the forest canopy during the Bosco Fontana measurement campaign and limits of detection (LoD, ppbv), based on 25-minute averages.

m/z	33	45	59	61	69	71	73	81
Compound	Methanol	Acetaldehyde	Acetone	Acetic acid	Isoprene	MVK+MACR	MEK	Monoterpenes
Max	14.6	3.44	7.31	14.9	4.79	1.95	1.05	0.419
Min	2.13	< LOD	1.18	0.396	< LOD	0.083	0.097	< LOD
Mean	6.16	1.46	3.24	1.92	1.07	0.506	0.454	0.198
Standard deviation	2.52	0.67	0.91	1.09	0.80	0.28	0.21	0.07
Median	5.69	1.30	3.14	1.73	0.934	0.506	0.428	0.199
1st Quartile	4.19	0.964	2.68	1.22	0.409	0.325	0.311	0.140
3rd Quartile	7.53	1.87	3.82	2.31	1.53	1.95	0.568	0.245
LOD	0.436	0.712	0.239	0.141	0.167	0.081	0.048	0.067

Table 3. Summary of the BVOC fluxes (mg m^{-2} h^{-1}) recorded during the Bosco Fontana field campaign based on 25-minute values. Values in brackets cover the campaign period where data is available from both instruments to enable direct comparison (15/06-06/07/2012 and 15/06-25/06/2012 for isoprene and monoterpenes, respectively).

m/z	33	45	59	61	69		71	73	81	
Compound	Methanol	Acetaldehyde	Acetone	Acetic acid	Isoprene PTR-MS	Isoprene PTR-ToF-MS	MVK + MACR	MEK	Monoterpenes PTR-MS	Monoterpenes PTR-ToF-MS
Max emission flux	0.492	0.436	0.585	0.328	9.867 (9.867)	9.195 (9.195)	0.641	0.181	0.478 (0.478)	0.609 (0.603)
Max deposition flux	-1.589	-0.335	-0.692	-0.876	-0.238 (-0.238)	-0.305 (-0.305)	-0.457	-0.128	-0.167 (-0.167)	-0.065 (-0.057)
1st Quartile	-0.032	-0.011	-0.029	-0.044	0.005 (0.005)	0.019 (0.019)	-0.012	-0.012	-0.009 (-0.008)	0.005 (0.001)
3rd Quartile	0.070	0.053	0.057	0.033	1.624 (1.796)	2.661 (2.661)	0.054	0.024	0.093 (0.101)	0.159 (0.137)
Mean	0.017	0.024	0.016	-0.007	0.961 (1.003)	1.465 (1.465)	0.025	0.009	0.056 (0.060)	0.098 (0.088)
Standard deviation	0.123	0.067	0.098	0.091	1.369 (1.387)	1.911 (1.911)	0.076	0.039	0.108 (0.111)	0.138 (0.134)
Median	0.010	0.013	0.008	0.000	0.168 (0.199)	0.410 (0.410)	0.011	0.005	0.020 (0.021)	0.036 (0.028)

Mean day-time flux (06:00-18:00)	0.033	0.045	0.030	0.001	1.912 (1.978)	2.917 (2.917)	0.049	0.018	0.117 (0.120)	0.206 (0.207)
Standard deviation	0.161	0.082	0.125	0.096	1.401 (1.383)	1.842 (1.842)	0.095	0.050	0.141 (0.129)	0.141 (0.144)
Median day-time flux (06:00-18:00)	0.038	0.044	0.026	0.001	1.635 (1.790)	2.905 (2.905)	0.041	0.014	0.090 (0.099)	0.192 (0.164)

Table 4. Non-exhaustive summary of isoprene fluxes recorded in the Mediterranean region and the isoprene emission factor under basal conditions (temperature: 30 °C and PAR: 1000 µmol m^{-2} s^{-1}).

Ecosystem	Dominant species	Season	Mean day time isoprene flux (mg m^{-2} h^{-1})	Isoprene emission factor under basal conditions (mg m^{-2} h^{-1})	Reference
Mixed oak and hornbeam forest	*Carpinus betulus* *Quercus robur*	Summer	2.6	1.7	This study
Oak forest	*Quercus pubescens*	Spring	2.8	7.4	Kalogridis et al. 2014
Oak forest	*Quercus pubescens*	Summer	5.4-10.1	5.4	Baghi et al. 2012
Mixed oak and pine forest	*Pinus pinea* *Quercus ilex* *Quercus suber*	Autumn	ca. 0.13	0.61	Fares et al. 2013

Table 5. Leaf level isoprene and monoterpene emission (mg m^{-2} h^{-1}) recorded using GC-MS from single leaves under basal conditions (temperature: 30 °C and PAR: 1000 µmol m^{-2} s^{-1}). ND signifies not detected.

Tree species	isoprene flux (standard error)	α-pinene flux (standard error)	sabinene flux (standard error)	β-pinene flux (standard error)	limonene flux (standard error)	sum monoterpene flux
Carpinus betulus	2.25×10^{-3} (1.50×10^{-3})	1.07×10^{-2} (6.00×10^{-3})	1.81×10^{-2} (1.36×10^{-2})	5.14×10^{-2} (1.23×10^{-2})	5.83×10^{-1} (2.36×10^{-1})	6.63×10^{-1}
Quercus robur	2.39×10^{0} (6.12×10^{-1})	2.81×10^{-2} (1.45×10^{-2})	ND	4.70×10^{-3} (3.08×10^{-3})	2.16×10^{-1} (6.49×10^{-2})	2.49×10^{-1}
Quercus rubra	9.14×10^{-1} (2.02×10^{-1})	ND	ND	7.95×10^{-3} (2.22×10^{-3})	2.34×10^{-2} (7.11×10^{-3})	3.13×10^{-2}
Corylus avellana	4.97×10^{-4} (3.93×10^{-4})	1.30×10^{-2} (8.00×10^{-3})	ND	2.08×10^{-2} (4.80×10^{-3})	7.57×10^{-1} (4.15×10^{-1})	7.90×10^{-1}
Acer campestre	4.40×10^{-4} (3.11×10^{-4})	5.14×10^{-2} (2.95×10^{-2})	ND	2.27×10^{-1} (3.54×10^{-2})	1.07×10^{-1} (1.41×10^{-2})	3.85×10^{-1}
Sambucus nigra	4.09×10^{-3} (3.66×10^{-3})	ND	ND	9.67×10^{-3} (2.69×10^{-3})	2.49×10^{-1} (1.41×10^{-1})	2.59×10^{-1}
Cornus sanguinea	4.00×10^{-1} (4.00×10^{-1})	1.11×10^{-3} (1.11×10^{-3})	ND	1.95×10^{-2} (4.91×10^{-3})	2.28×10^{-1} (1.73×10^{-1})	2.49×10^{-1}

Table 6. Species specific isoprene and monoterpene emission factors (for a standard temperature of 30 °C and a PAR value of 1000 µmol m^{-2} s^{-1}). Values derived from optimising the leaf level emission factors to give the best fit with the measured above canopy isoprene and monoterpene fluxes within the constraints displayed.

Species	Isoprene emission factor (mg m^{-2} h^{-1})	Isoprene constraint (mg m^{-2} h^{-1})	Monoterpene emission factor (mg m^{-2} h^{-1})	Monoterpene constraint (mg m^{-2} h^{-1})
Acer campestre	0.00	< 1.0	0.15	< 0.50
Acer negundo	0.00	< 1.0	0.33	< 0.64
Alnus glutinosa	0.01	< 1.0	0.22	< 0.50
Carpinus betulus	0.00	< 1.0	0.57	< 0.63
Corylus avellana	0.00	< 1.0	0.23	< 0.50
Fraxinus angustifolia	0.00	< 1.0	0.00	< 0.50
Juglans nigra	0.00	< 1.0	0.12	< 0.50
Juglans regia	0.36	< 1.0	0.15	< 0.50
Morus sp.	0.00	< 1.0	0.19	< 0.50
Platanus hispanica	2.97	< 4.4	0.50	< 0.50
Populus × canescens	10.66	< 16.1	0.29	< 0.50
Populus × hybrida	8.06	< 16.1	0.00	< 0.50
Prunus avium	0.00	< 1.0	0.01	< 0.50
Quercus cerris	0.02	< 1.0	0.07	< 0.50
Quercus robur	7.46	< 16.1	0.19	< 0.50
Quercus rubra	1.38	< 8.1	0.02	< 0.50
Robinia pseudoacacia	1.38	< 2.8	0.01	< 0.50
Rubus sp.	0.00	< 1.0	0.01	< 0.50
Tilia sp.	0.00	< 1.0	0.00	< 0.50
Ulmus minor	0.01	< 1.0	0.01	< 0.50
Grass	0.06	< 1.0	0.06	< 0.15
Not woodland	0.06	< 1.0	0.08	< 0.15
Outside forest	0.06	< 1.0	0.06	< 0.50

Figure 1. Time series of meteorological conditions recorded over the campaign period. From top to bottom: PAR (µmol m^{-2} s^{-1}), air temperature (°C), relative humidity (%), wind speed (m s^{-1}) and wind direction (°).

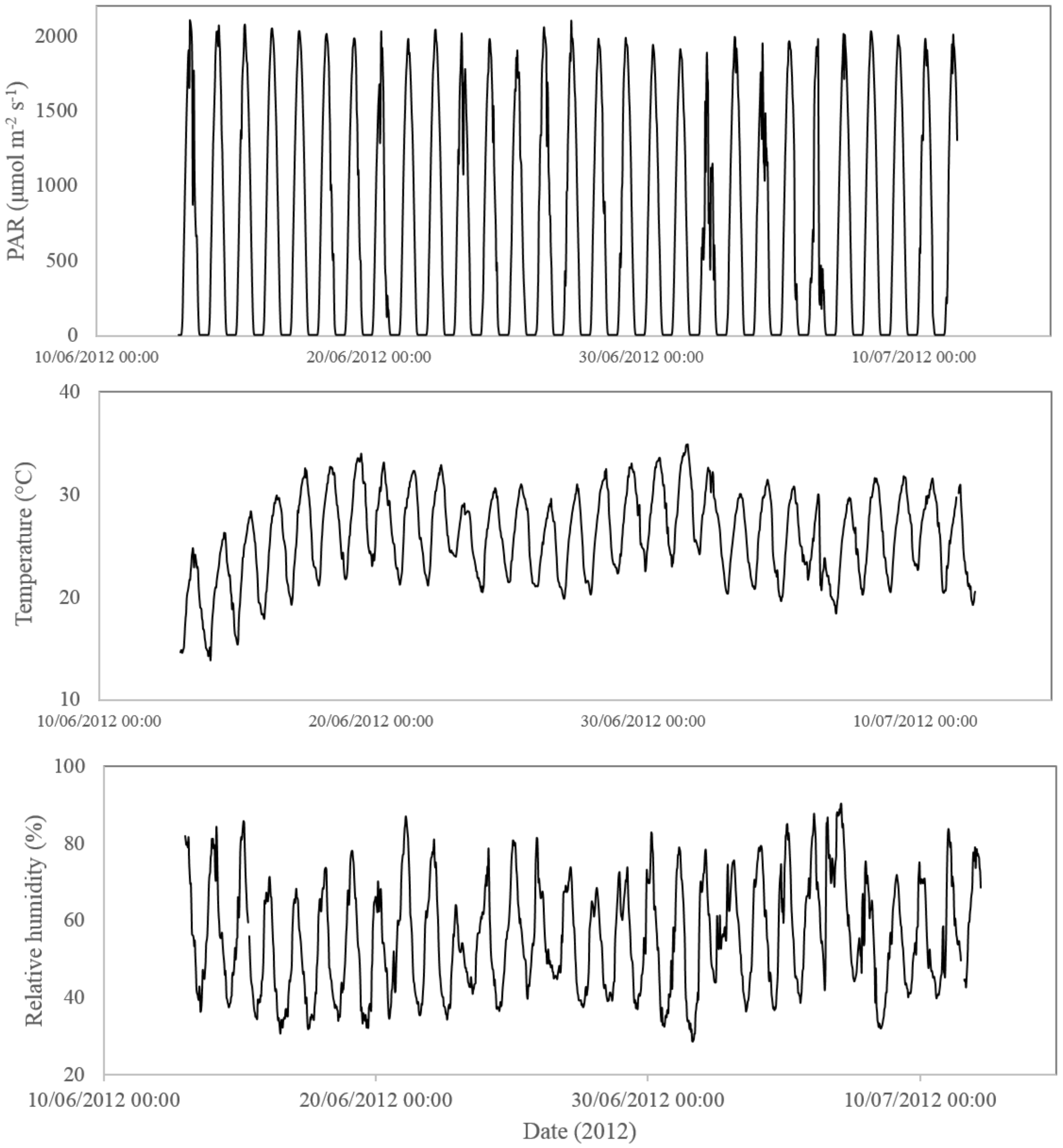

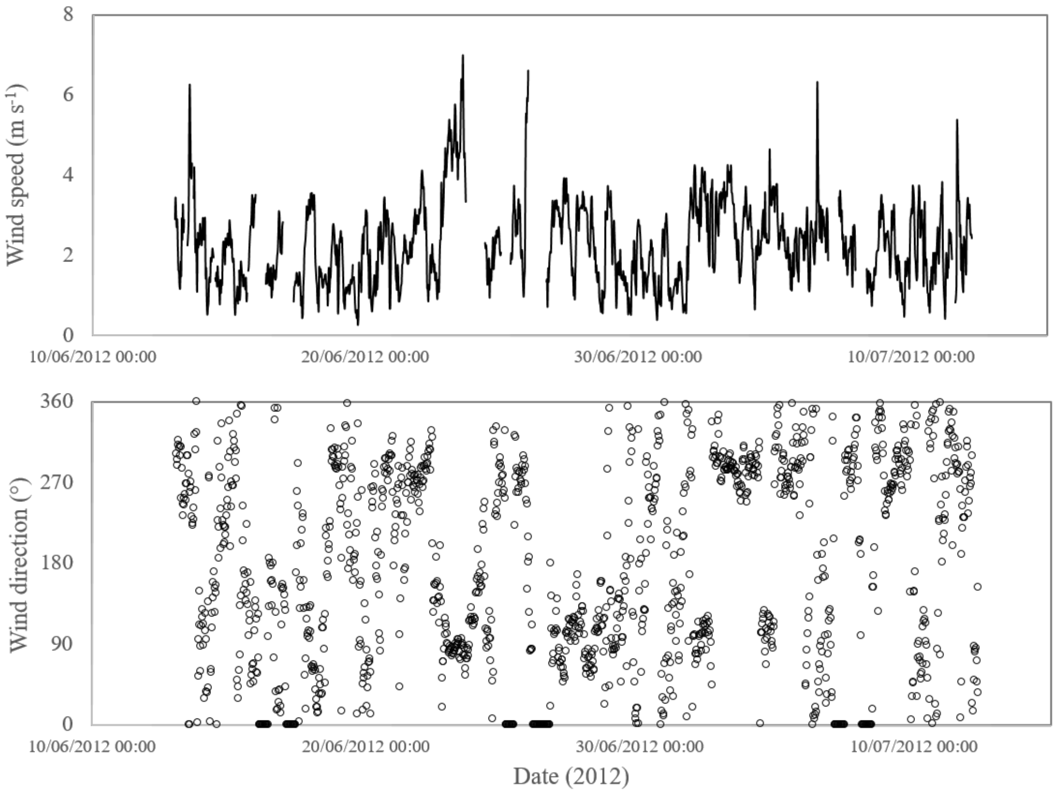
Wind speed (m s-1)
8
6
4
2
0
10/06/2012 00:00
20/06/2012 00:00
30/06/2012 00:00
10/07/2012 00:00
Wind direction (°)
360
270
180
90
0
10/06/2012 00:00
20/06/2012 00:00
30/06/2012 00:00
10/07/2012 00:00
Date (2012)

Figure 2 Satellite image (map data © Google 2016) of the field site showing flux tower and the campaign average (13/06/2012 – 11/07/2012) flux footprint representing 80 % of the total flux.

Figure 3. Mean 4 m above-canopy diurnal mixing ratios by volume of volatile organic compounds measured during the Bosco Fontana field campaign. Error bars represent one standard deviation from the mean and the dashed line denotes limit of detection.

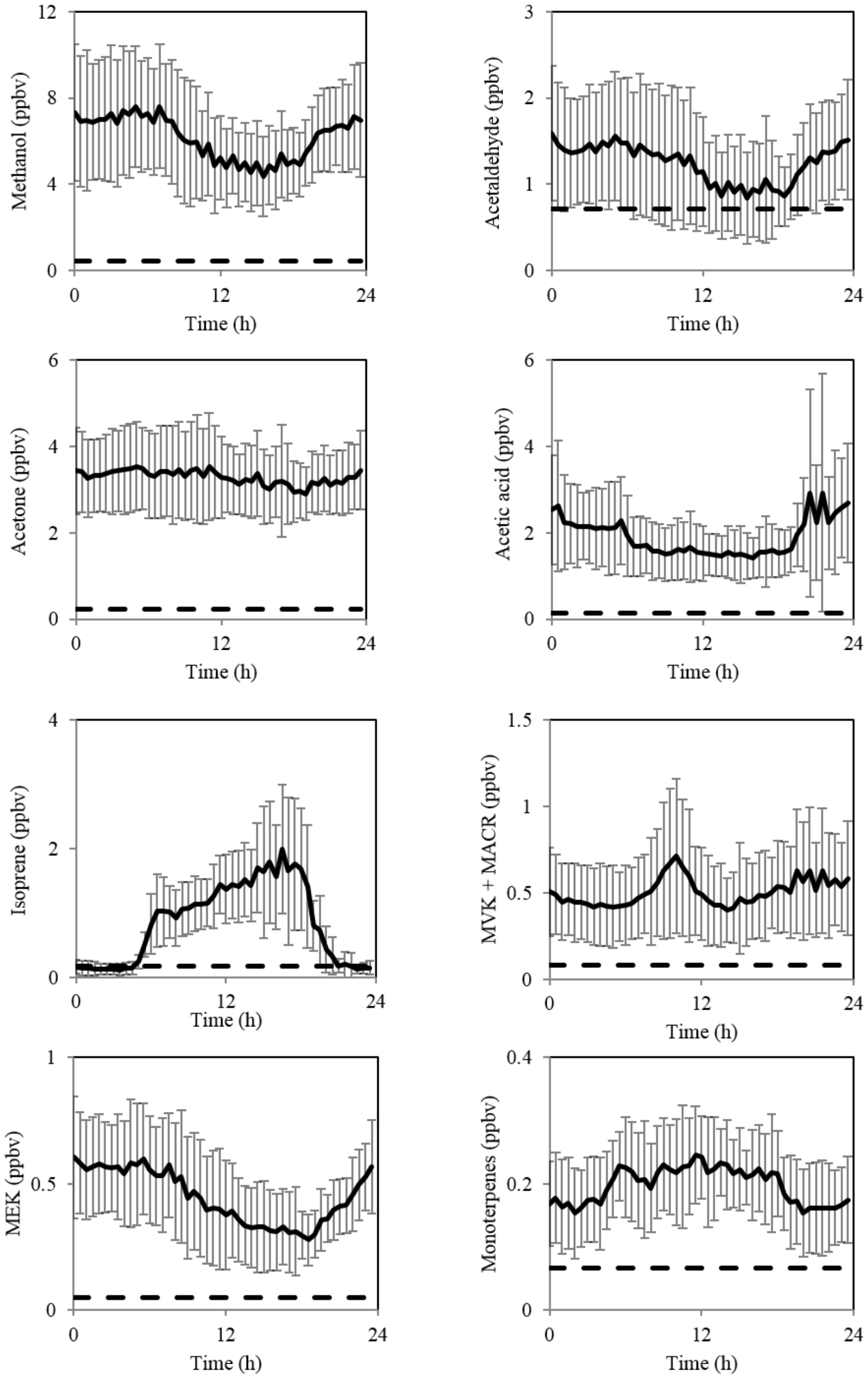

Figure 4. Time series of isoprene (top) and monoterpene (middle) fluxes (mg m^{-2} h^{-1}) measured using vDEC. 25 min averaged flux data from the PTR-MS which passed all tests, fell below the u$_*$ threshold and fell below the LoD are represented by blue circles, triangles and diamonds respectively. Red circles and lines represent PTR-ToF-MS isoprene and monoterpene fluxes with 30 min averaged flux files failing the stationarity test removed. Bottom, scatter plot showing the relationship between isoprene fluxes calculated using PTR-MS and PTR-ToF-MS.

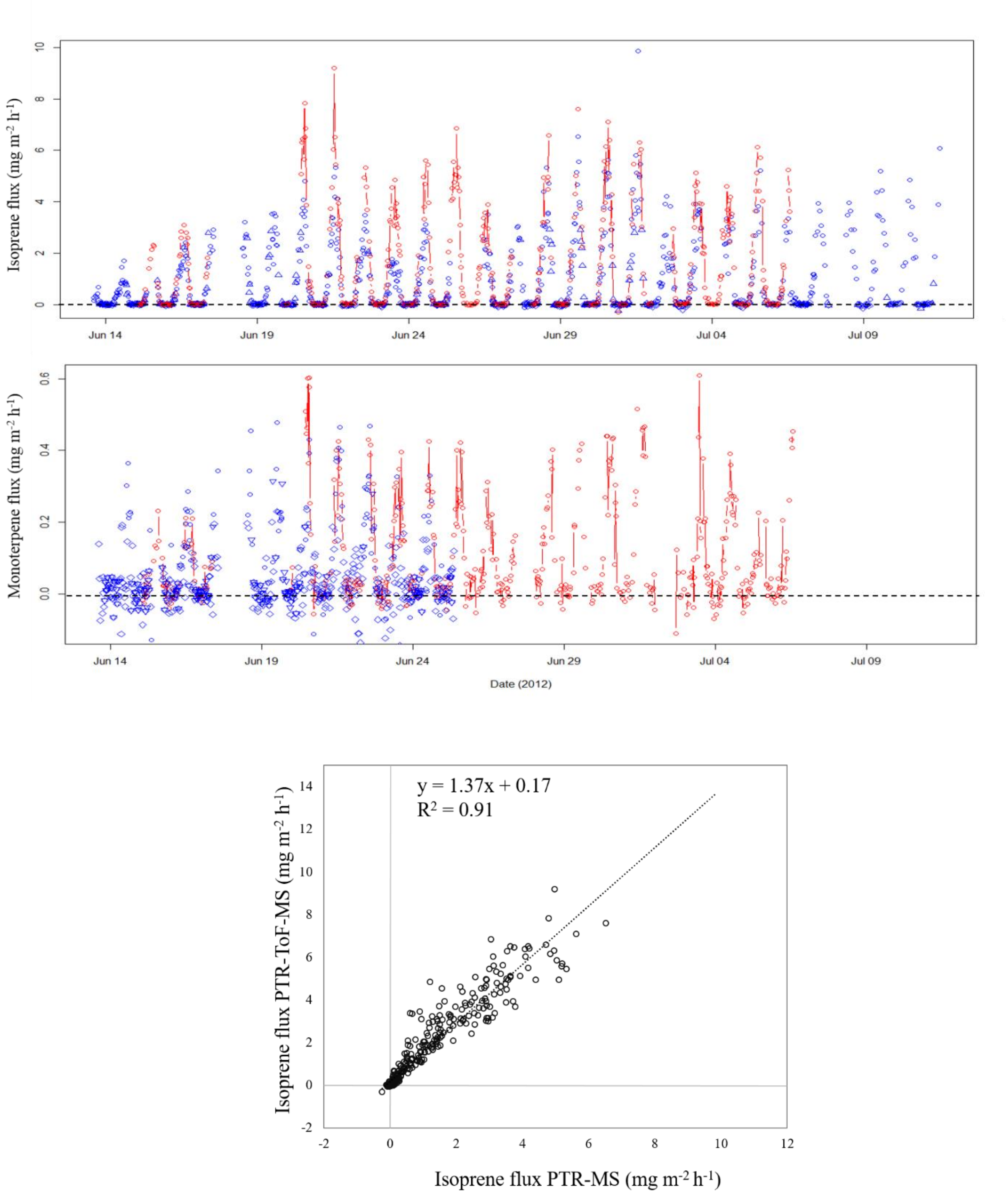

Figure 5. Mean diurnal fluxes of volatile organic compounds measured using vDEC. Shaded area represents the limit of detection of the averaged data, and error bars represent one standard deviation between days from the mean.

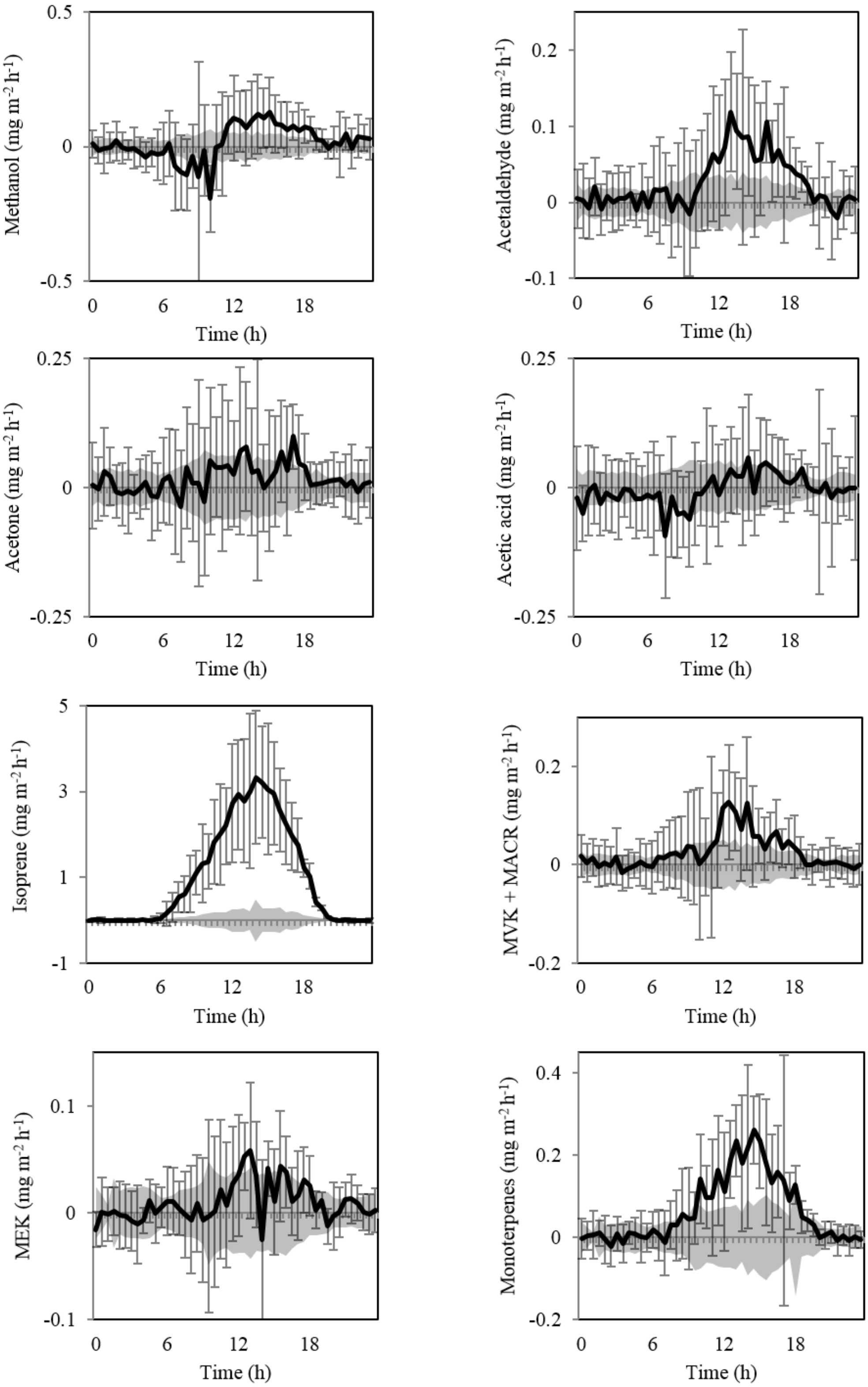

Figure 6. Comparison of PTR-MS (blue) and PTR-ToF-MS (red) mass scans relative to *m/z* 59 at unit mass resolution averaged between 14th and 24th June. Compounds recorded in flux mode using the PTR-MS are presented in black with compounds tentatively identified in grey.

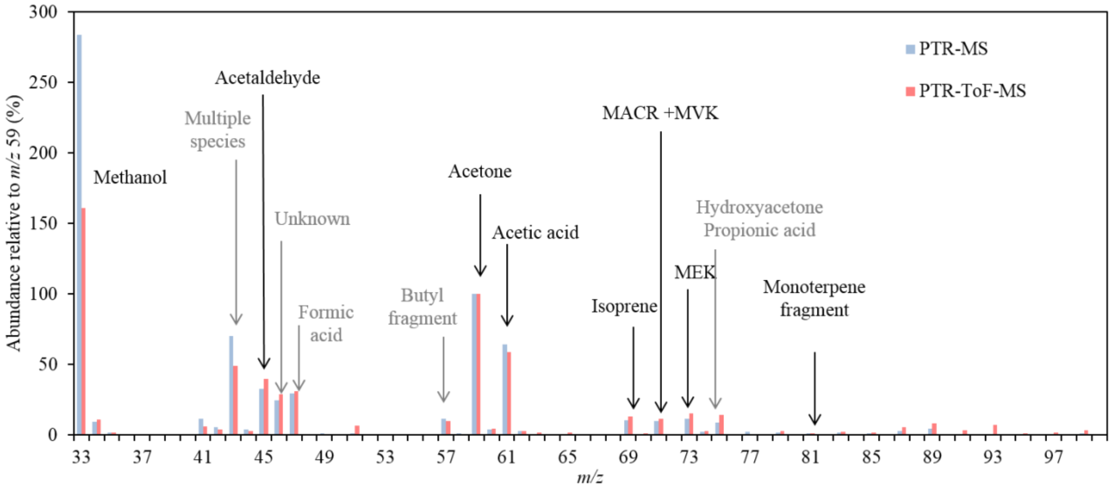

Figure 7. Scatter plots displaying the relationship between the mixing ratios by volume of methanol, acetone and MEK measured 4 m above the canopy, coloured by temperature.

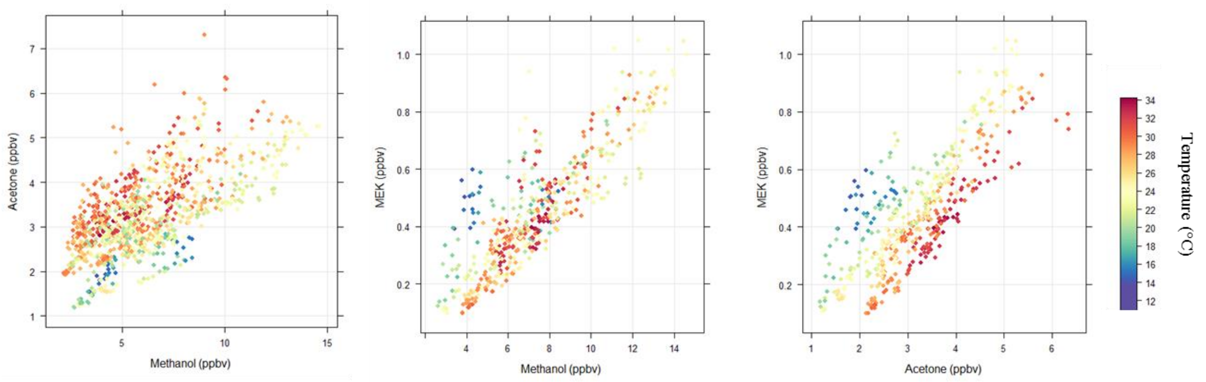

Figure 8. The relationship between temperature (°C) and isoprene fluxes (mg m^{-2} h^{-1}) and mixing ratios (ppbv), coloured according to the magnitude of photosynthetically active radiation (µmol m^{-1} s^{-1}).

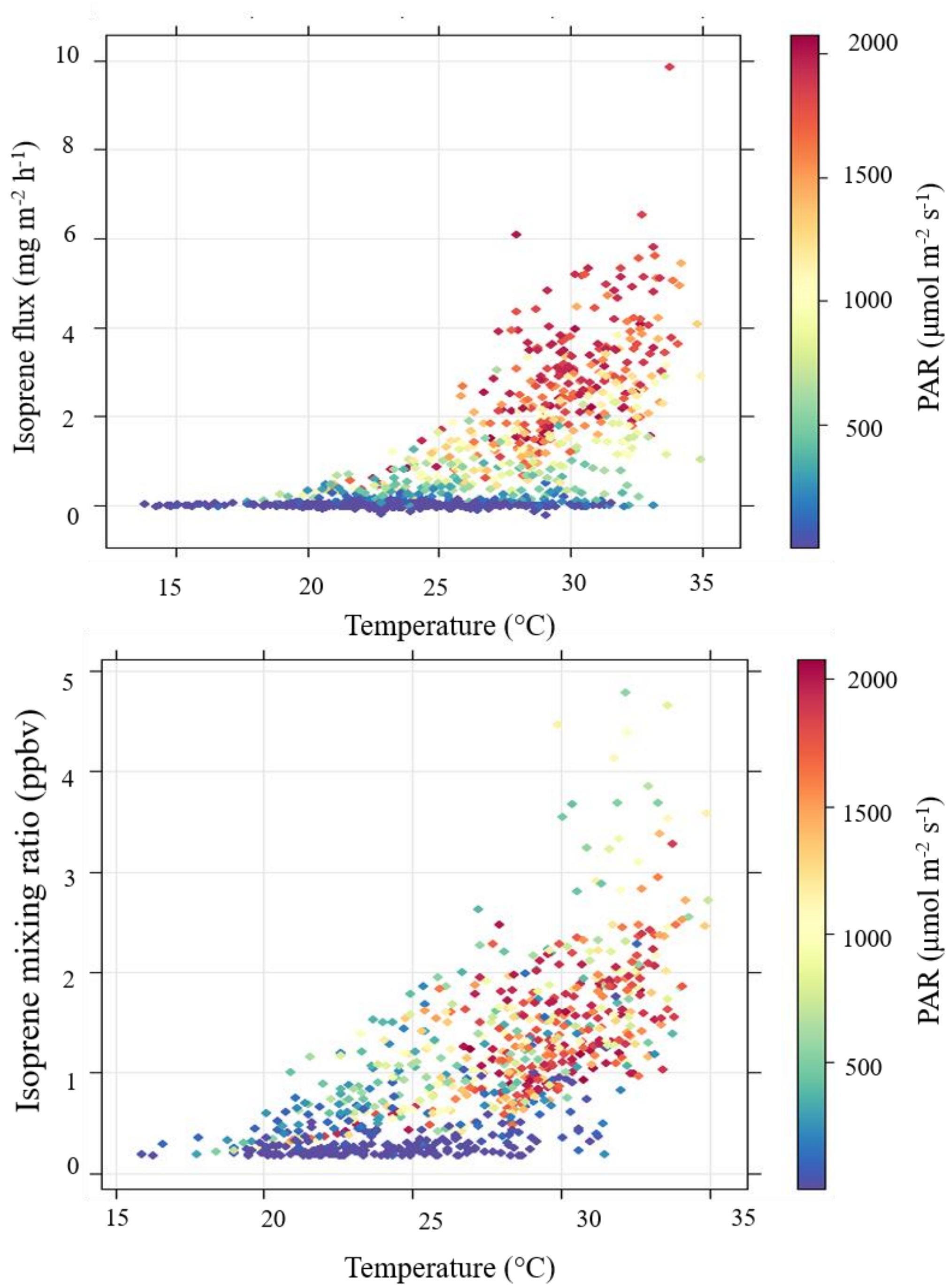

Figure 9. Measured isoprene fluxes against the product of γ (emission activity factor, itself the product of the temperature, light and leaf area index activity factors) and ρ (the canopy loss and production factor).

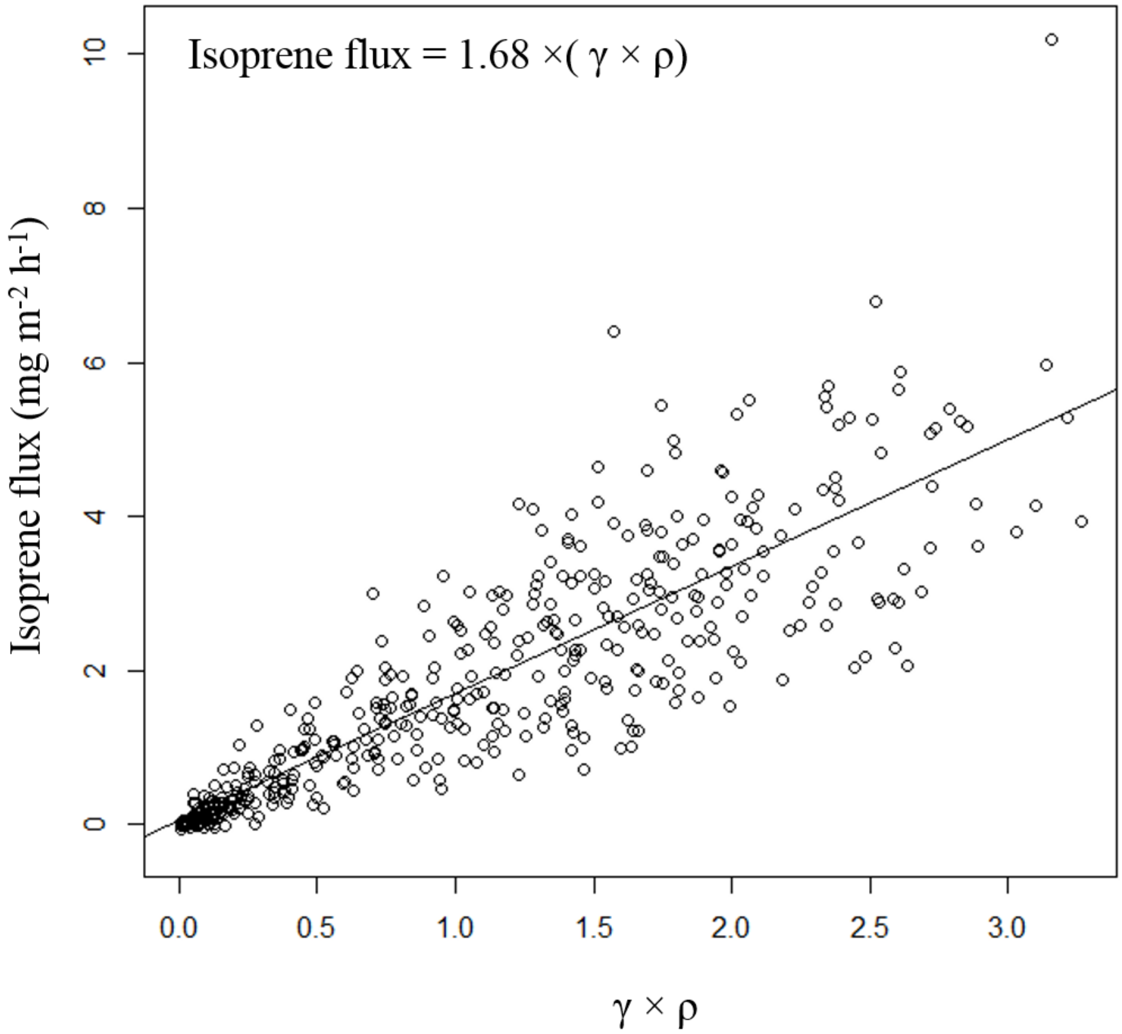

Figure 10 Plot of the residual values from the temperature only monoterpene emission model against PAR, demonstrating that light as well as temperature has a significant impact on monoterpene emissions.

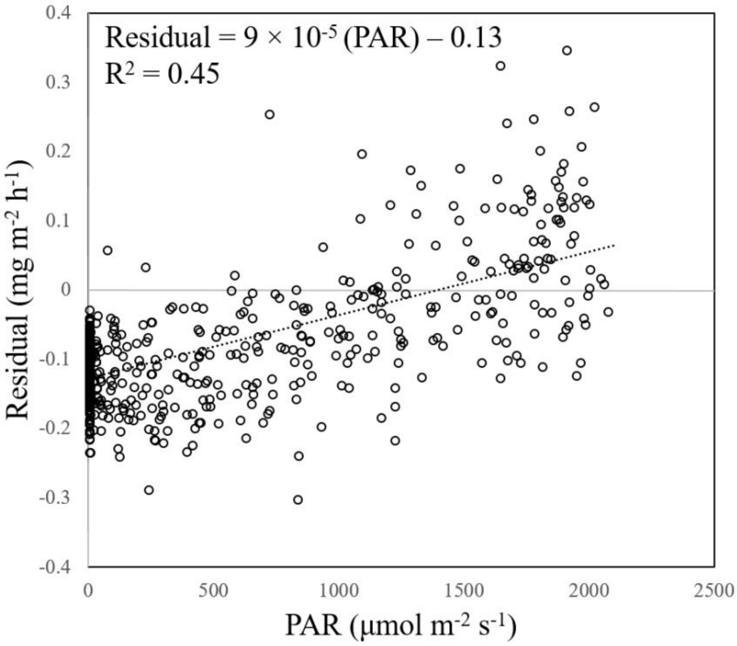

Figure 11 The contribution of individual tree species to the speciated isoprene and monoterpene flux on the 2nd July 2012. PAR is displayed as a yellow line, wind direction as a black line and the flux recorded using the PTR-MS as bold black bars.

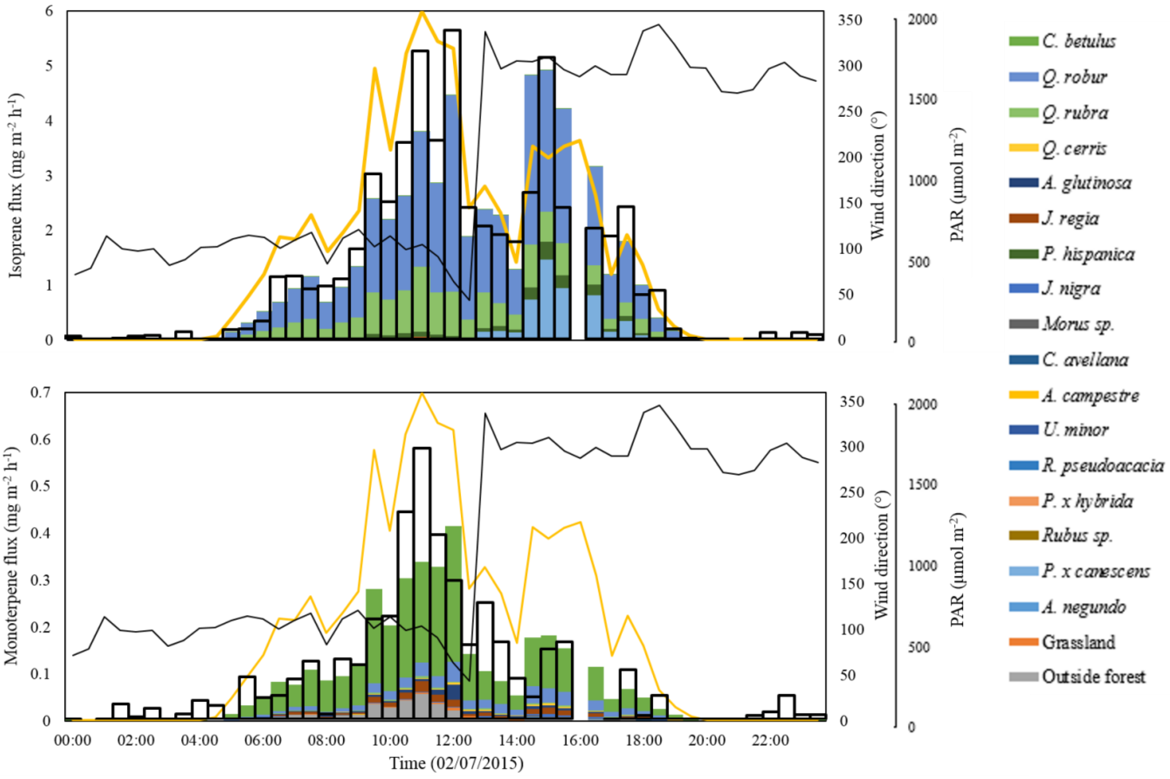

Supplementary material for “Canopy-scale flux measurements and bottom-up emission estimates of volatile organic compounds from a mixed oak and hornbeam forest in northern Italy”

1 Virtual disjunct eddy covariance lag time determination

The lag time between the measurement of vertical wind speed and concentration measurements using PTR-MS were calculated by identifying the absolute maximum value of the covariance function within a 30 s time window (MAX method, Taipale et al. 2010). Points for which the noise to signal ratio was greater than one were substituted for a flux calculated using a fixed lag time to prevent an overestimation of the flux from the MAX method. A histogram of isoprene lag times calculated using the MAX method is displayed in Figure S1. This histogram shows a clear maximum at 7.5 s, hence 7.5 s was taken to be the fixed isoprene lag time and lag times of other masses measured were calculated from this value ± the instrumental dwell time.

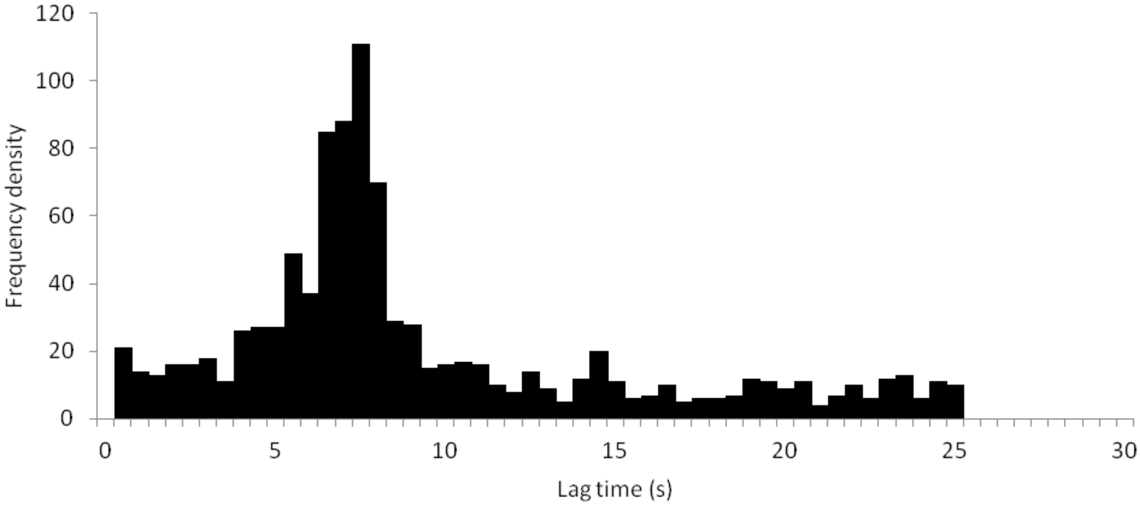

Figure S1. Histogram of isoprene lag times calculated using the MAX method

2 Assessment of the underestimation of total flux through the loss of low frequency fluxes

The loss of low frequency fluxes caused by the rotation of coordinates in order to set the mean vertical wind velocity to zero for each 25 minute averaging period is assessed in Figure S2. Sensible heat flux data were averaged over 50, 75, 100 and 125 minutes before coordinate rotation and plotted against the sum of two, three, four and five 25 minute coordinate rotated flux files respectively. The flux lost from the use of 25 minute averaging periods can be estimated from the gradient of the fitted line between the two fluxes. Eddies with a time period between 25 and 125 minutes were shown to carry an additional 2.8 % of the sensible heat flux. Therefore assuming that the frequency of VOC and sensible heat fluxes are comparable, 1.0-3.6 % of the VOC flux is lost by limiting the averaging period to 25 minutes.

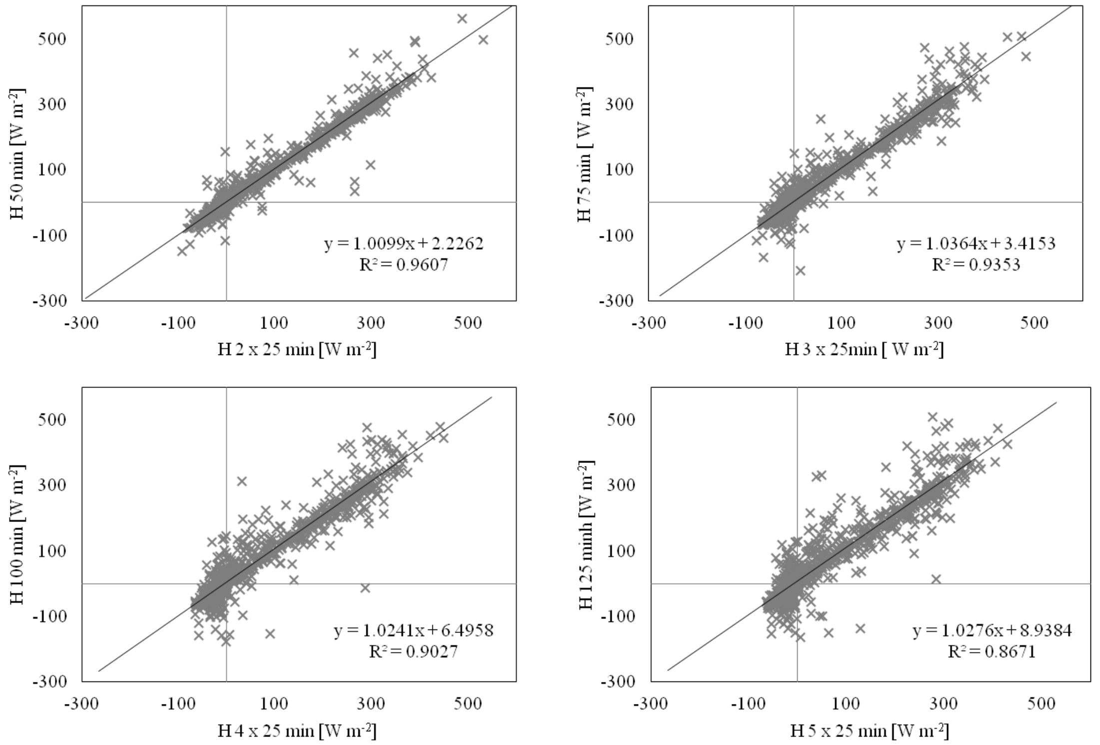

Figure S2. Plots of sensible heat flux (H) determined over differing averaging times during the intensive field campaign at Bosco Fontana. Solid line represents the best linear fit.

3 The uncertainty caused by disjunct eddy covariance

The uncertainty caused by disjunct eddy covariance was estimated by comparing the sensible heat flux (*H*) calculated using eddy covariance with *H* calculated using temperature measurements taken every 4.9 s. Figure S3 shows the correlation between H measured using eddy covariance and disjunct eddy covariance, as is shown the uncertainty introduced by disjunct sampling is 0.17 %.

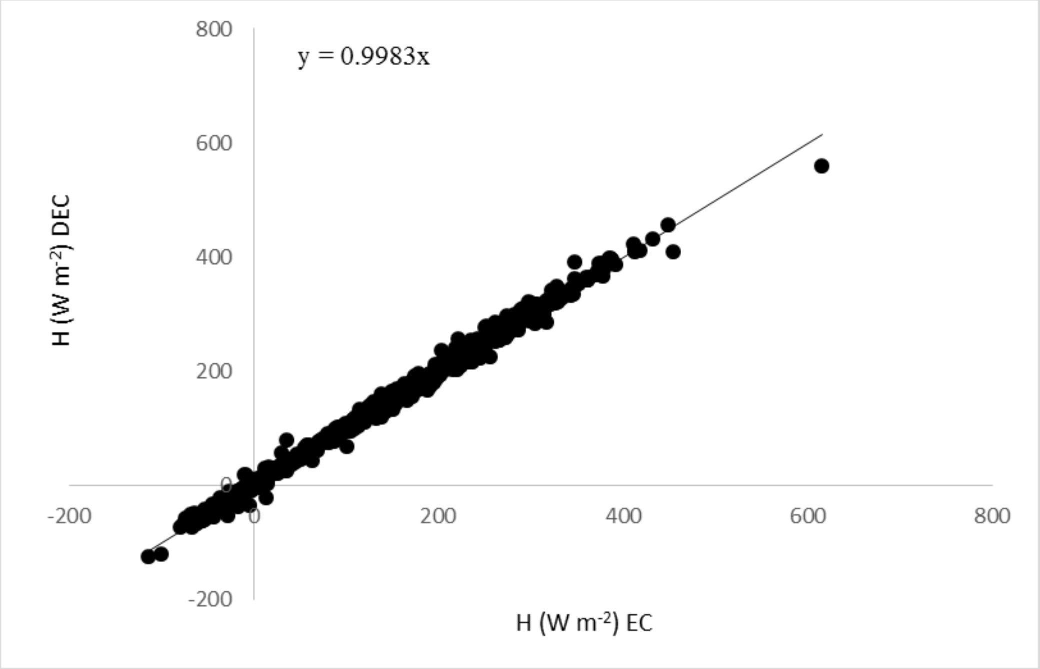

Figure S3. Sensible heat flux calculated (H) calculated using eddy covariance (EC) and disjunct eddy covariance (DEC).

4 Flux quality assessment

Each 25 min VOC flux file calculated from the PTR-MS data using the virtual disjunct eddy covariance (vDEC) method was subjected to three quality tests, each performed independently (Langford et al., 2010a). Flux files were flagged if they the mean frictional velocity over the 25 min averaging period dropped below 0.15 m s^{-1}, if they dropped below the limit of detection (Wienhold et al., 1994) or if they failed a stationarity test (Foken and Wichura, 1996). The percentage of flux files passing or failing these tests is summarised in Table S1 for each compound measured. In addition the percentage of the flux footprint falling outside the forest was assessed for each flux file with 26 % of files having > 25 % of flux from outside the forest area.

Table S1. Summary of flux quality assessment test results

Compound	Turbulence test failed ($u_* < 0.15$ m s^{-1})	25 minute Limit of detection test failed (F < LOD)	Stationarity test fail ($\Delta s > 60\%$)	Passed all tests
Methanol (*m/z* 33)	29 %	60 %	6 %	25 %
Acetaldehyde (*m/z* 45)	29 %	74 %	3 %	18 %
Acetone (*m/z* 59)	29 %	82 %	3 %	11 %
Acetic acid (*m/z* 61)	29 %	70 %	7 %	14 %
Isoprene (*m/z* 69)	29 %	36 %	2 %	50 %
MVK + MACR (*m/z* 71)	29 %	78 %	3 %	15 %
MEK (*m/z* 73)	34 %	85 %	1 %	7 %
Monoterpenes (*m/z* 81)	34 %	74 %	0 %	19 %

5. The effect of the tower on atmospheric flow

The measurement tower was a large structure so could conceivably impact on atmospheric flow and therefore flux measurements. In order to assess the impact of the tower on flux files θ, the rotation angle used to realign measurements of u and w was plotted against wind direction (Fig. S4, top). The measurement tower located to the south east of the sonic anemometer does not appear to significantly affect θ.

The effect of wake turbulence from the tower on the flux measurements was assessed using the method developed by Foken (2004). The integral turbulence statistics of the vertical wind velocity ($\sigma_w/u*$, the standard deviation of the vertical wind velocity normalised by the friction velocity) of each flux file were compared with $\sigma_w/u*$ calculated for an ideal set conditions. The percentage difference between the measured and modelled data was then used to assess the overall data quality. This percentage difference plotted against wind direction is displayed in Fig. S4 (bottom). As can be seen the wind direction has little effect on the percentage difference indicating that the tower does not impact upon the flux measurements.

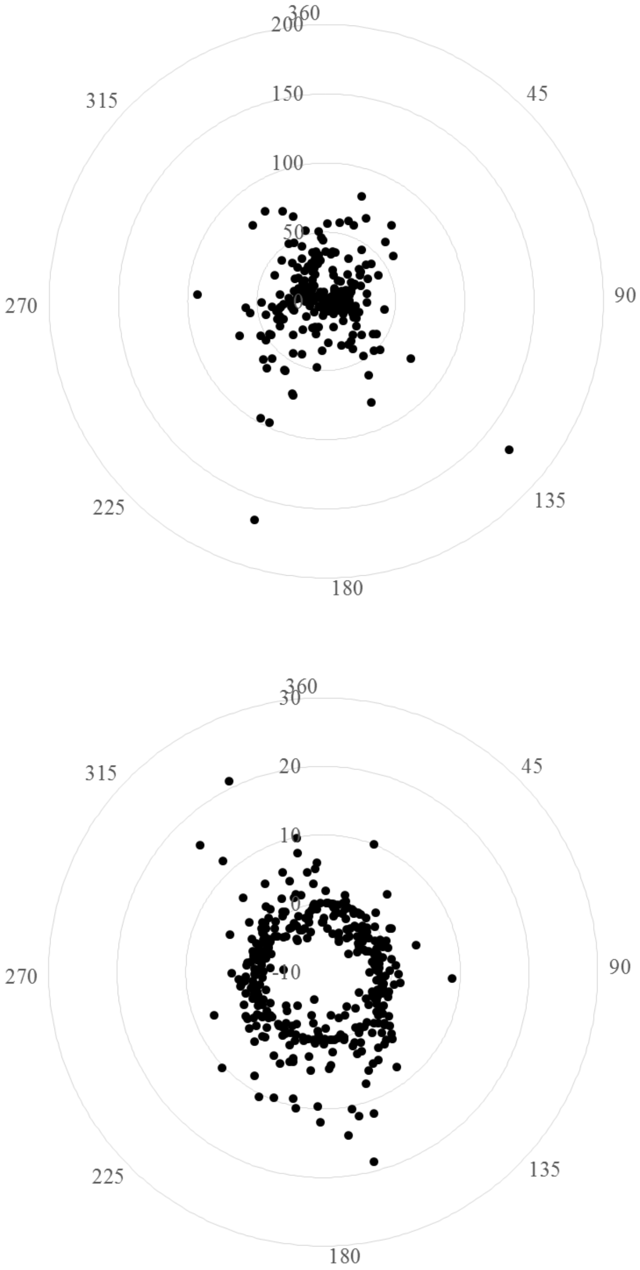

Figure S4 Wind rose plots showing the effect of wind direction (°) on the rotation angle (θ) required to set w to zero (top) and the % difference between the measured and modelled turbulence statistic (bottom).

6 Leaf surface temperature

The leaf surface temperature was estimated by extrapolation of ambient temperature using the resilience approach described by Nemitz *et al.* (2009). Figure S5 shows the diurnal patterns of average ambient and leaf surface temperature. At night average leaf surface temperature was found to be approximately 2 °C below the average ambient air temperature, during the day average leaf surface temperature peaked approximately 10 °C above the average ambient air temperature.

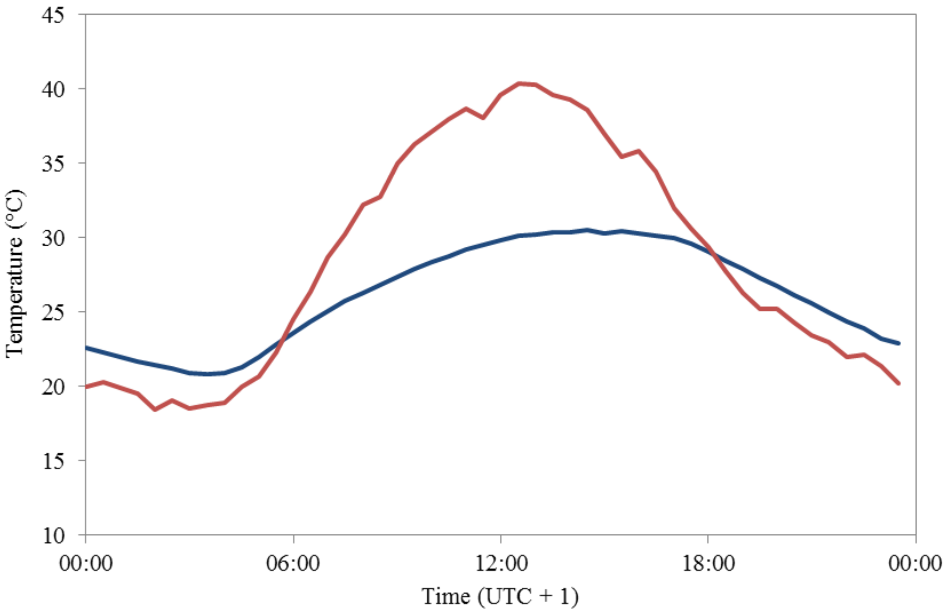

Figure S5. The diurnal pattern of average ambient temperature recorded 4 m above the canopy (blue) and leaf surface temperature (red).

6 Discussion of flux measurements

The fluxes and mixing ratios of the 8 masses monitored using the PTR-MS instrument during the field campaign at Bosco Fontana are discussed in more detail below.

6.1 Methanol (*m/z* 33)

The mass spectral peak at *m/z* 33 is commonly assigned to methanol (Misztal et al., 2011, Rinne et al., 2005) and published GC-PTR-MS measurements did not reveal any other significant contribution to this mass (de Gouw and Warneke, 2007). Here *m/z* 33 has been assigned to methanol, there may be some contribution to *m/z* 33 the O_2H^+ cluster ion but this should be removed in the background subtraction.

Methanol emission is of interest to atmospheric science and has been shown to have a significant effect on tropospheric oxidants (Tie et al., 2003). However, uncertainties in surface emission estimates result in significantly different model predictions of atmospheric oxidants (Jacob et al., 2005; Millet et al., 2008; Tie et al., 2003). Methanol fluxes have been recorded above temperate woodland (Karl et al., 2003; Park et al., 2013; Rinne et al., 2007; Spirig et al. 2005) and agricultural ecosystems (Custer and Schade 2007; Ruuskanen et al., 2011). The methanol mixing ratios recorded over the course of this study are displayed in Figure S6. Methanol was the most abundant compound recorded during the campaign with a mean mixing ratio of 6.2 ppbv over the campaign which is comparable to the results obtained by Sprig et al. (2005) above a mixed European deciduous forest. The diurnal profile of the methanol mixing ratio is shown in Figure 6, it can be seen that mixing ratios are stable through the night at ca. 7 ppbv and drop to a low of ca. 5 ppbv in the mid-afternoon, most probably caused by expansion of the planetary boundary layer. The flux of methanol peaked at 0.49 mg m^{-2} h^{-1} with a mean day-time flux of 0.03 mg m^{-2} h^{-1} (Figure 5). Methanol deposition was observed in the mornings followed by a rapid increase in methanol emission in the late morning peaking in the early afternoon, a similar emission pattern of morning deposition followed by afternoon emission was observed by Langford et al. (2010a) and Misztal et al. (2011) above tropical rain forest and oil palms in South East Asia.

Biogenic methanol emission stems from a number of sources the largest of which is the demethylation of pectin in the primary cell walls (Galbally and Kirstine, 2002; Fall 2003). The strong temperature dependence of emissions reported previously (Hayward et al., 2004; Custer and Schade, 2007) indicates enzymatically driven emission or release from stored pools (inside the leaf or in water on the leaf surface). However, this was not observed in this study (data not shown suggesting that emission directly resulting from the enzymatically controlled demethylation of pectin is unlikely to be the sole source of methanol at this site. Other possible sources of methanol include emissions from decaying biomatter (Warneke et al., 1999; Grey et al., 2010) and as a result of herbivore feeding on the local vegetation and other wounding events (von Dahl et al., 2006; Arneth and Niinemets, 2010).

As a result of its low Henry's law constant methanol can be lost from atmosphere through precipitation, wet deposition and dry deposition (Riemer et al., 1998; Seco et al., 2007). While the rain immediately preceding measurements and on the 6th of July corresponded with a period of lower methanol mixing ratios no drop was observed immediately following rainfall. This suggested that lower methanol mixing ratios were not caused by the rain event but by air mass change prior to the rain itself as shown by Schade and Goldstein (2006). There is also evidence (Asensio et al., 2007) that soil may act as a sink of bVOCs, this may therefore also be a contributing factor to the methanol deposition observed in the mornings but from our findings it is impossible to determine whether the sink driving the downwards flux was the soil, plant surfaces (wet or dry), the stomata or a combination of the above.

6.2 Acetaldehyde (*m/z* 45)

The signal measured at *m/z* 45 was attributed to acetaldehyde, while there may be a small contribution at this nominal mass from CO_2 this was corrected for by background subtraction. It has been reported that acetaldehyde may be formed as an artefact following the reaction of ozone with impurities in the inlet line (de Gouw and Warneke, 2007) but no correlation was observed between ozone and acetaldehyde so this is not thought to be a significant source of acetaldehyde in these measurements.

Together with formaldehyde, methanol and acetone, acetaldehyde is one of the major oxygenated volatile organic compounds in the atmosphere and plays a significant role in atmospheric chemistry (Andrews et al., 2012; Millet et al., 2010). Acetaldehyde emission has previously been reported from woodland (Karl et al., 2002; Karl et al., 2003) and grassland (Custer and Schade, 2007; Ruuskanen et al., 2011), and the close proximity of the forest at Bosco Fontana to urban areas means that a contribution from anthropogenic sources to the observed ambient concentrations is also likely (Langford et al., 2009; Langford et al., 2010b). Acetaldehyde mixing ratios above the Bosco Fontana nature reserve peaked at 3.4 ppbv from a mean value of 1.5 ppbv, a time series of acetaldehyde mixing ratios is displayed in Figure S6. The acetaldehyde daily profile, shown in Figure 3, shows a stable night time mixing ratio of ca. 1.5 ppbv dropping to ca. 1 ppbv in the mid-to-late afternoon. The daily mean acetaldehyde flux is displayed in Figure 5. While the peak acetaldehyde flux was recorded at 0.44 mg m^{-2} h^{-1} the daily maximum was usually ca 0.12 mg m^{-2} h^{-1}. The daily flux profile shows that emission fluxes increased until the early afternoon before stabilizing and then decreasing to zero in the evening. This represents a lower emission flux than reported previously from both a pine canopy (Rinne et al., 2007) and mixed forest (Karl et al., 2003). This may be related to the relatively small area of the forest at Bosco Fontana as the surrounding farmland is unlikely to contribute significantly to the acetaldehyde flux (Custer and Schade, 2007).

Millet et al. (2010) recently used the GEOS-Chem atmospheric chemistry model to identify acetaldehyde sources and sinks, identifying hydrocarbon oxidation as the largest acetaldehyde source. Both isoprene and monoterpenes have been identified as acetaldehyde precursors (Lee et al., 2006; Luecken el al., 2012), no correlation was seen between acetaldehyde and isoprene mixing ratios over the canopy at Bosco Fontana but a weak correlation ($R^2 = 0.27$) was observed between acetaldehyde and monoterpene mixing ratios. As well as formation from hydrocarbon oxidation, acetaldehyde is also directly emitted by plants in response to wounding (Brilli et al., 2011; Loreto et al., 2006) and via ethanolic fermentation in leaves and roots subject to anoxic conditions (Fall, 2003; Seco et al., 2007; Winters et al., 2009). In addition to emission from plants Schade and Goldstein (2001) also determined that soil and litter emission of acetaldehyde contributed significantly to the canopy-scale flux. As well as acting as a source of acetaldehyde into the atmosphere it has been shown that some tree species may act as an acetaldehyde sink at high ambient concentrations (Rottenberger et al., 2005; Seco et al., 2007). However, significant net deposition fluxes were not observed in this campaign.

The correlation between acetaldehyde and monoterpene mixing ratios indicates that there is likely to be a significant contribution from hydrocarbon oxidation to the acetaldehyde mixing ratio. However, the early afternoon peak in acetaldehyde flux coupled with no correlation with ozone suggests that the observed flux is predominantly of biogenic origin and most probably originates from ethanolic fermentation in leaves and soil.

6.3 Acetone (*m/z* 59)

The mass spectral peak observed at *m/z* 59 may be attributed to acetone or propanal. However, previous studies have indicated that contribution of propanal to this mass is low, 0-10 %, (de Gouw and Warneke, 2007) therefore *m/z* 59 is here attributed to acetone.

Acetone is one of the most abundant oxygenated VOCs in the atmosphere and fluxes of acetone have been recorded over both anthropogenic (Langford et al., 2009; Langford et al., 2010b) and woodland environments (Karl et al., 2002; Karl et al., 2003). Acetone may also play a significant role in tropospheric chemistry as it can act as a source of HOx radicals in the upper troposphere leading to increased ozone production (Singh et al., 1995).

At the Bosco Fontana site acetone was the second most abundant volatile recorded after methanol, the mixing ratio remained constant throughout the day (Figure 3) with a mean value of 3.2 ppbv. This value was higher than mixing ratios previously observed over hardwood forest where average mixing ratios have been reported in the range of 1.2-1.9 ppbv (Kalogridis et al., 2014; Karl et al., 2003) but comparable to mixing ratios recorded over ponderosa pine (Goldstein and Schade, 2000). No significant acetone flux was observed at night, the flux appeared to increase in the afternoon but remained below the LoD throughout the day (Figure 5). The mean day-time emission of 0.03 mg m^{-2} h^{-1} was significantly lower than that observed by Karl et al. (2003) above a mixed hardwood forest.

Acetone is produced in the atmosphere through the oxidation of VOC precursors (Jacob et al., 2002; Lee et al., 2006). It is also emitted directly by plants into the atmosphere via a number of pathways, for example acetone is produced as a by-product of cyanogenesis and is then released into the atmosphere (Fall, 2003). Acetone may also be produced by acetoacetate decarboxyation in the soil (Fall, 2003). While Jacob et al. (2002) found emission from plant decay inconsistent with the seasonal cycle observed at European sites, Karl et al. (2003) reported emission from decaying biomass based on the emission factors calculated by Warneke et al. (1999). Enhanced acetone emission is also commonly reported following plant wounding events (Davison et al., 2008; Ruuskanen et al., 2011).

6.4 Acetic acid (*m/z* 61)

The mass spectral peak observed at *m/z* 61was assigned to acetic acid, this is supported by de Gouw et al. (2003) who observed a correlation between *m/z* 61 and acetic acid. This mass spectral peak, assigned to acetic acid, has been detected previously over a Mediterranean oak forest (Kalogridis et al., 2014).

The dominant source of acetic acid in the troposphere is the photochemical oxidation of biogenically emitted hydrocarbons (Glasius et al., 2001; Lee et al., 2006, Paulot et al., 2011), and the direct emission of acetic acid into the atmosphere is comparatively low. However, acetic acid is emitted into the atmosphere by vegetation (Seco et al., 2007) with emission shown to be predominantly from tree species rather than crop plants (Kesselmeier et al., 1998). Emission is triggered by light (Kesselmeier et al., 1998; Staudt et al., 2000) and has been seen to correlate with transpiration (Kesselmeier et al., 1998; Seco et al., 2007). Acetic acid emission has also been recorded following stress events such as cutting (Ruuskanen et al., 2011) and herbivory (Bartolome et al., 2007; Llusià J. and Peñuelas, 2001; Scutareanu et al., 2002).

Field-scale emission of acetic acid from *Citrus sinensis* L. was observed by Staudt et al. (2000) in the noon and afternoon with deposition occurring in the early morning and night. Sinks of acetic acid include wet deposition and dry deposition with wet deposition the most important sink (Paulot et al., 2011). Photochemical losses are low as acetic acid may be considered as the final product of the photo-oxidation of many BVOCs. Kuhn et al. (2002) hypothesised that the primary control on acetic acid uptake by plants was the ambient mixing ratio and that a mixing ratio compensation point exists. When acetic acid mixing ratios are above this compensation point acetic acid will be absorbed by plants and when ambient mixing ratios drop below this point acetic acid will be emitted. Soil may also act as an acetic acid sink with uptake of acetic acid by a Mediterranean forest soil observed by Asensio et al. (2007). Deposition of acetic acid has been reported both over tropical forests (Karl et al., 2004; Langford et al., 2010a) and pine woodland (Karl et al., 2005), but fluxes of acetic acid over temperate deciduous woodland have yet to be reported.

During the Bosco Fontana campaign the acetic acid mixing ratios dropped in the early morning and remained relatively stable at ca. 1.5 ppbv throughout the day before rising again to ca. 2.5 ppbv, in the evening (Figure 3). This likely corresponded to the changing height of the planetary boundary layer. In the latter half of the campaign a large increase in mixing ratio was observed at ca. 21:00 each day peaking at 14.9 ppbv on the 29th June (Figure S6), these spikes correspond to a northerly wind direction but no source could be identified. The acetic acid flux was low but appears to show a pattern similar to that observed by Staudt et al. (2000) with deposition observed in the morning followed by emission in the afternoon (see Figure 5). The change from acetic acid deposition to emission occurs when the ambient mixing ratio drops below ca.1.9 ppbv which is within the compensation point range calculated by Kuhn et al. (2002) for tropical tree species but no conclusions can be drawn with confidence from such a weak flux.

6.5 Isoprene (*m/z* 69)

Isoprene measurements using the PTR-MS mass spectral peak at *m/z* 69 have been shown to agree with GC-MS measurements (Kuster et al., 2004). Isoprene fluxes recorded using PTR-MS have been reported previously from temperate forest canopies (for example Karl et al., 2003) and given the clear diurnal cycle of *m/z* 69 fluxes and mixing ratios (Figures 3 and 5) coupled with the presence of two significant isoprene emitting species (*Quercus robur* and *Quercus rubra*). In the Bosco Fontana forest canopy *m/z* 69 was assigned to isoprene. Interferences from furan, associated with biomass burning, as well as a number of BVOCS, in particular 2-methyl-3-buten-2-ol (MBO) have previously been reported at *m/z* 69 (de Gouw and Warneke, 2007). While large concentrations of MBO have been observed over coniferous forests in the USA (Goldan et al., 1993) emission has not been reported from European deciduous species and as biomass burning in the Italian summer is low a significant contribution from these species at *m/z* 69 was considered to be unlikely.

Four tree species: *Carpinus betulus, Quercus robur, Quercus rubra* and *Quercus cerris* (Dalponte et al., 2007) make up ca. 75 % of the Bosco Fontana canopy, and of these only *Quercus robur* and *Quercus rubra* are known to emit isoprene (Pérez-Rial et al., 2009; Pier, 1995). Owing to isoprene emission only occurring during the day time coupled with a short atmospheric lifetime both mixing ratios and fluxes peaked in the afternoon, with fluxes peaking ca. 2 h before mixing ratios and dropping to zero at night. At the Bosco Fontana field site large day-to-day variations in the daily maximum isoprene mixing ratios (ppbv) and fluxes were observed due to changing environmental conditions. Isoprene mixing ratios (ppbv) peaked in the late afternoon with maximum values ranging from 0.8 ppbv to 4.8 ppbv (Figure S6). The mean above canopy isoprene mixing ratio (1.1 ppbv) was comparable to that observed by Karl et al. (2003) above a North American hardwood forest but lower than the 1.2 ppbv observed by Kalogridis et al. (2014) above a French oak forest. This is to be expected given that 90 % of this canopy was made up of the isoprene emitting species *Quercus pubescens*. In addition, Bosco Fontana represents a relatively small area of isoprene emitting vegetation in mainly agricultural surroundings, with low isoprene emissions, possibly with the exception of some fields of poplar plantations. This implies that, as local isoprene emissions shut off at night, low-isoprene air is advected into the forest, giving rise to lower night-time concentration that found in extensive isoprene emitting areas.

The mean day-time isoprene flux, 1.91 mg m^{-2} h^{-1}, was higher than that observed by Laffineur et al. (2011) over a European temperate mixed forest but lower than the flux reported by Spirig et al. (2005) and Kalogridis et al. (2014) over European mixed broadleaf and oak forests, respectively.

6.6 MVK and MACR (*m/z* 71)

The structural isomers MVK and MACR are both detected at *m/z* 71 when analysed using PTR-MS. Analysis using PTR-MS only enables compound identification on the basis of nominal mass so it is not possible to separate these species, and for this reason together with their common chemical origin, they will be treated together here. Previous studies have shown good agreement between PTR-MS and GC-MS measurements of MVK+MACR (de Gouw et al., 2003) although a significant contribution from crotonaldehyde at this mass has also been reported (Karl et al., 2007).

MVK and MACR are the main products formed following the first stage of isoprene oxidation in the atmosphere (Atkinson and Arey 2003a), accounting for 80 % of the carbon. Isoprene oxidation predominantly occurs via reaction with OH during the day and with NO_3 at night with a relatively small contribution from ozone (Monks et al., 2009). It has been proposed that isoprene oxidation to MVK and MACR may occur within the plant (Jardine et al., 2012; Llusià et al., 2011) as well and the atmosphere. MACR can also be directly produced within plants as a biproduct in the production of cyanogenic glycosides (Fall, 2003). Once formed MVK and MACR may undergo further atmospheric oxidation and photochemical reactions (Millet et al., 2010; Atkinson and Arey, 2003b) or be deposited onto the canopy (Karl et al., 2010).

Fluxes and mixing ratios of MVK and MACR have previously been reported over deciduous forests (Apel et al., 2002; Kalogridis et al., 2014; Spirig et al., 2005). Above the canopy of the Bosco Fontana natural reserve a positive flux of MVK + MACR (Figure 5) was observed peaking in the early afternoon with a day-time mean flux of 0.05 mg m^{-2} h^{-1}, suggesting significant within canopy oxidation of isoprene. This value is comparable to that observed by Spirig et al. (2005) over a European deciduous forest. The flux of MVK + MACR dropped below the limit of detection at night which was expected as isoprene mixing ratios fell to ca. 0 ppb overnight (Figure 3). As with previous campaigns over European deciduous forest no clear evidence for deposition was observed (Kalogridis et al., 2014; Spirig et al., 2005), this is in contrast to measurements over more remote tropical forests where deposition is usually reported (Karl et al., 2004; Langford et al., 2010a; Misztal et al., 2011). This suggests that deposition of these species to the forest canopy is low and that these species are lost through atmospheric transportation or undergo further reaction prior to being deposited. At the Bosco Fontana natural reserve, this is likely to be driven by the high oxidative capacity of the Po valley atmosphere. The mean MVK and MACR mixing ratio observed was 0.51 ppbv.

6.7 MEK (*m/z* 73)

The mass observed at *m/z* 73 was assigned here to methyl ethyl ketone (MEK), however the isomeric compound butanal could also contribute to this signal (Table 1). Previous studies have shown a quantitative agreement between PTR-MS and GC analysis of MEK at *m/z* 73 (Davison et al., 2008; de Gouw et al., 2006) but measurement is complicated by the humidity dependent background contribution from $H_3O^+(H_2O)_3$.

MEK can be emitted directly from some plant species as a by-product of hydrogen cyanide production from lotaustralin (Fall, 2003). MEK emission has predominantly been reported following plant wounding events such as grass cutting (Davison et al., 2008; Karl et al., 2001; Llusià et al., 2011) and insect herbivory (Peñuelas et al., 2005; Pinto et al., 2007). As well as direct emission MEK may also be formed photochemically (Luecken et al., 2012). MEK has been recorded over oak (Kalogridis et al., 2014) and coniferous forests (Müller et al., 2006), with mixing ratios peaking at 0.15-0.51 ppbv and 1.8 ppbv respectively. Above the canopy at Bosco Fontana MEK mixing ratios fell between these values peaking at 1.0 ppbv (Figure 3). MEK mixing ratios peaked at night before dropping to a low in the late afternoon, most likely caused by dilution in the expanding planetary boundary layer. Fluxes of MEK have not been reported in the literature and few of the flux files from this campaign passed the quality tests, the daily averaged flux (Figure 5), however, showed a low emission of MEK in the afternoon with a mean day-time flux of 0.02 mg m^{-2} h^{-1}.

6.8 Monoterpenes (*m/z* 81)

Measurement of monoterpenes using PTR-MS is complicated by the differing fragmentation patterns of the numerous monoterpene species, however monoterpenes are commonly measured using PTR-MS at *m/z* 137 and 81 corresponding to the protonated parent ion and a principle fragment ion respectively (de Gouw and Warneke, 2007). Owing to poor instrumental sensitivity at higher atomic mass units (amus) the monoterpene fluxes and mixing ratios reported here are calculated from *m/z* 81. While there could be some contribution from sesquiterpene and hexenal fragment ions at this mass, previous studies have demonstrated that this signal can be assigned to monoterpenes (de Gouw et al., 2003; Rinne et al., 2005). Variability in the ratio between parent and fragment ions was limited by ensuring the *E/N* ratio was held constant throughout the measurements period.

Many plant species, including the four dominant species in the Bosco Fontana canopy, have been shown to emit monoterpenes (Isebrands et al., 1999; König et al., 1995; Owen et al., 2001; Pérez-Rial et al., 2009). Monoterpenes are emitted from plants both directly and from stored pools such as glandular trichomes and resin ducts (Maffei, 2010). Emission is driven by temperature (Tarvainen *et al.,* 2005) and also occurs as a response to both biotic (Copolovici et al., 2011; Peñuelas et al., 2005) and abiotic (Kaser et al., 2013; Llusià et al., 2002) stress. As well as emission from plants, low levels of monoterpene emission have also been reported from litter and soil (Gray et al., 2010; Hayward et al., 2001; Leff and Fierer, 2008).

Above the Bosco Fontana forest canopy monoterpene fluxes peaked in the early afternoon with a mean day-time flux of 0.12 mg m^{-2} h^{-1} (Figures 4 and 5) which is comparable to the flux observed by Spirig et al. (2005) above a European mixed deciduous forest but much lower than those observed by Davison et al. (2009) over a macchia ecosystem in western Italy. As was observed by Spirig et al. (2005) the monoterpene flux dropped to ca. 0 mg m^{-2} h^{-1} at night. Laffineur et al. (2011) detected a weak temperature dependent monoterpene flux at night over a mixed European forest, this discrepancy may be due to larger emission from monoterpenes stored in pools from the coniferous species present in the mixed forest. While monoterpene deposition has previously been observed (Bamberger et al.2011) no net deposition was observed above the canopy at Bosco Fontana. The monoterpene mixing ratios followed a diurnal cycle with values peaking at ca. 0.2 ppbv at mid-day, dropping to ca. 0.18 ppbv at night (Figures 3 and 4). The mean monoterpene mixing ratio observed (0.2 ppbv) was much higher than the 0.06 ppbv observed by Kalogridis et al. (2014) over a Mediterranean oak forest but were within the 0.13-0.30 ppbv range of values recorded by Davison et al. (2009) and comparable to the mixing ratios observed by Spirig et al. (2005).

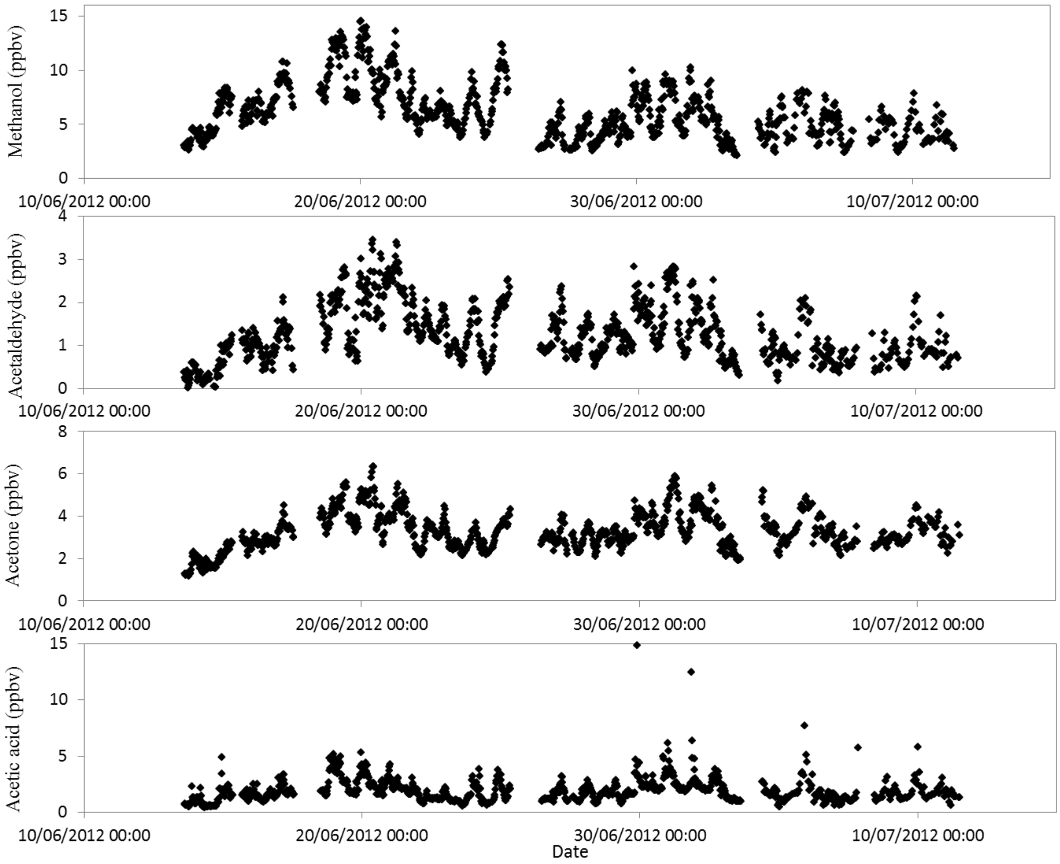
Methanol (ppbv)
15
10
5
0
Acetaldehyde (ppbv)
4
3
2
1
0
Acetone (ppbv)
8
6
4
2
0
Acetic acid (ppbv)
15
10
5
0
10/06/2012 00:00
20/06/2012 00:00
30/06/2012 00:00
10/07/2012 00:00
Date

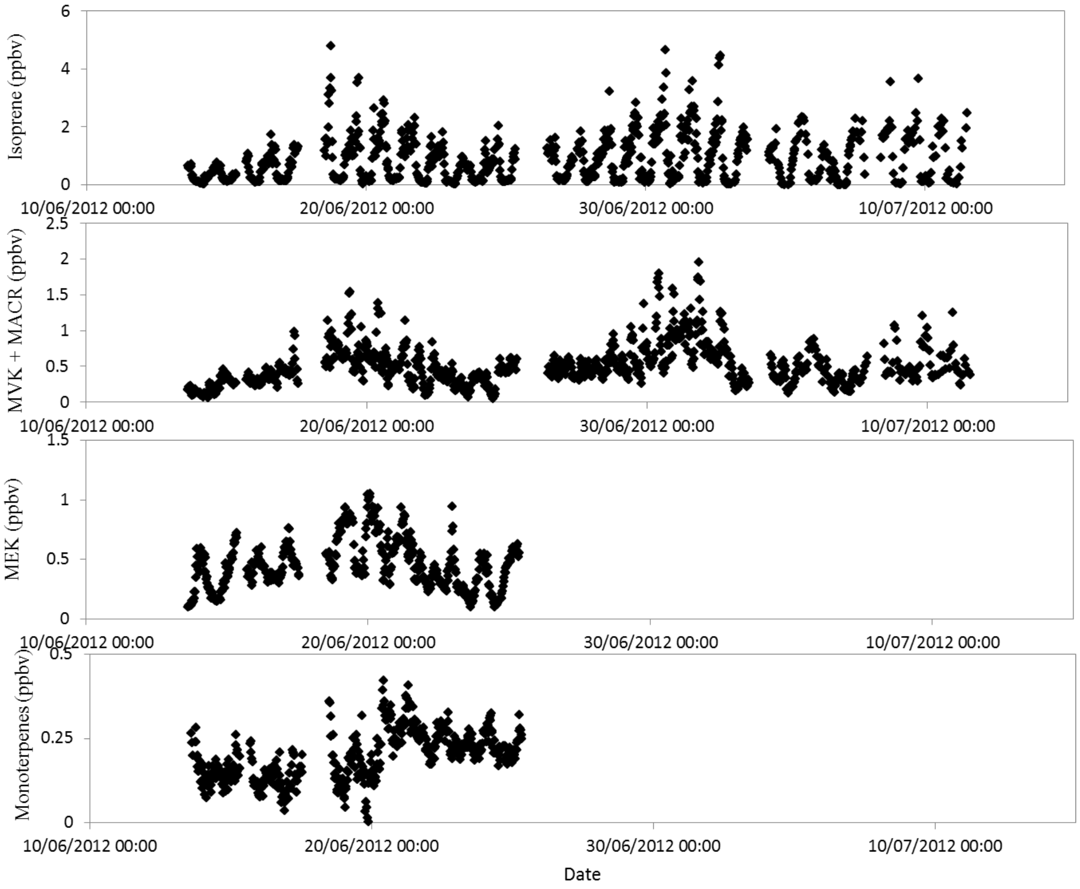
Isoprene (ppbv)
6
4
2
0
MVK + MACR (ppbv)
2.5
2
1.5
1
0.5
0
MEK (ppbv)
1.5
1
0.5
0
Monoterpenes (ppbv)
0.5
0.25
0
10/06/2012 00:00
20/06/2012 00:00
30/06/2012 00:00
10/07/2012 00:00
Date

Figure S6. Time series of the mixing ratios by volume of methanol, acetaldehyde, acetone, acetic acid, isoprene, MVK & MACR, MEK and monoterpene (calculated from fragment at *m/z* 81) measured at 4 m above the forest canopy

References

Andrews D. U., Heazlewood B. R., Maccarone A. T., Conroy T., Payne R. J., Jordan M. J. T. and Kable S. H.: Photo-tautomerization of acetaldehyde to vinyl alcohol: a potential route to tropospheric acids. Science, 337, 1203-1206, 2012.

Apel E.C., Riemer D.D., Hills A., Baugh W., Orlando J., Faloona I., Tan D., Brune W., Lamb B., Westberg H., Carroll M.A., Thornberry T. and Geron C.D.: Measurement and interpretation of isoprene fluxes and isoprene , methacrolein , and methyl vinyl ketone mixing ratios at the PROPHET site during the 1998 Intensive. Journal of Geophysical Research, 107, 4034, 2002.

Arneth A. and Niinemets Ü.: Induced BVOCs: How to bug our models? Trends in Plant Science, 15, 118–125, 2010.

Asensio D., Peñuelas J., Filella I. and Llusià, J.: On-line screening of soil VOCs exchange responses to moisture, temperature and root presence. Plant and Soil, 291, 249-261, 2007.

Atkinson R. and Arey J.: Gas-phase tropospheric chemistry of biogenic volatile organic compounds: a review. Atmospheric Environment, 37, 197-219, 2003a.

Atkinson R. and Arey J.: Atmospheric Degradation of Volatile Organic Compounds Roger. Chemical Reviews, 103, 4605-4638, 2003b.

Bamberger I., Hörtnagl L., Ruuskanen T.M., Schnitzhofer R., Müller M., Graus M., Karl T., Wohlfahrt G. and Hansel A.: Deposition fluxes of terpenes over grassland. Journal of Geophysical Research, 116, 1-13, 2011.

Bartolome J., Penuelas J., Filella I., Llusia J., Broncano M. J. and Plaixats J.: Mass scans from a proton transfer mass spectrometry analysis of air over Mediterranean shrubland browsed by horses. Journal of Environmental Biology, 28, 697-700, 2007.

Brilli F., Ruuskanen T.M., Schnitzhofer R., Müller M., Breitenlechner M., Bittner V., Wohlfahrt G., Loreto F. and Hansel A.: Detection of plant volatiles after leaf wounding and darkening by proton transfer reaction "time-of-flight" mass spectrometry (PTR-TOF). PloS one, 6, e20419, 2011.

Copolovici L., Kännaste A., Remmel T., Vislap V. and Niinemets Ü.: Volatile emissions from Alnus glutionosa induced by herbivory are quantitatively related to the extent of damage. Journal of Chemical Ecology, 37, 18-28, 2011.

Custer T. and Schade G.: Methanol and acetaldehyde fluxes over ryegrass. Tellus, 59, 673–684, 2007.

Dalponte M., Gianelle D. and Bruzzone L.: Use of hyperspectral and LIDAR data for classification of complex forest areas. Canopy Analysis and Dynamics of a Floodplain Forest: 25-37, 2007.

Davison B., Brunner A., Ammann C., Spirig C., Jocher M. and Neftel A.: Cut-induced VOC emissions from agricultural grasslands. Plant Biology, 10, 76-85, 2008.

Davison B., Taipale R., Langford B., Misztal P., Fares S., Matteucci G., Loreto F., Cape J.N., Rinne J. and Hewitt C.N.: Concentrations and fluxes of biogenic volatile organic compounds above a Mediterranean macchia ecosystem in western Italy. Biogeosciences, 6, 1655-1670, 2009.

de Gouw J.A., Warneke C., Stohl A., Wollny A.G., Brock C.A., Cooper O.R., Holloway J.S., Trainer M., Fehsenfeld F.C., Atlas E.L., Donnelly S.G., Stroud V. and Lueb A.: Volatile organic compounds composition of merged and aged forest fire plumes from Alaska and western Canada. Journal of Geophysical Research, 111, D10303, 2006.

de Gouw J. and Warneke C.: Measurements of volatile organic compounds in the earth's atmosphere using proton transfer-reaction mass spectrometry. Mass Spectrometry Reviews, 26, 223-257, 2007.

Fall R.: Abundant Oxygenates in the Atmosphere: A Biochemical Perspective. Chemical reviews, 103, 4941-4951, 2003.

Galbally I.E. and Kirstine W.: The Production ofMethanol by Flowering Plants and the Global Cycle of Methanol. Journal of Atmospheric Chemistry 43, 195–229, 2002.

Glasius M., Boel C., Bruun N., Easa L.M., Hornung P., Klausen H.S., Klitgaard K.C., Lindeskov C., Moller C.K., Nissen H., Petersen A.P.F., Kleefeld S., Boaretto E., Hansen T.S., Heinemeier J. and Lohse C.: Relative contribution of biogenic and anthropogenic sources to formic and acetic acids in the atmospheric boundary layer. Journal of Geophysical Research, 106, 7415-7426, 2001.

Foken, T. and Wichura, B.: Tools for quality assessment of surface- based flux measurements. Agricultural and Forest Meteorology, 78, 83–105, 1996.

Foken T., Göckede M., Mauder M., Mahrt L., Amiro B., and Munger W.: Post-field data quality control, in: Handbook of Micrometeorology: A guide for surface flux measurement and analysis, edited by: Lee, W. M. X. and Law, B., Dordrecht, Kluer Academic Publishers, 29, 181–203, 2004.

Goldan P.D., Kuster W.C., Fehsenfeld F.C. and Montzka S.A.: The observation of a C_5 alcohol emission in a North American pine forest. Geophysical Research Letters, 20, 1039-1042, 1993.

Goldstein A.H. and Schade G.W.: Quantifying biogenic and anthropogenic contributions to acetone mixing ratios in a rural environment. Atmospheric Environment, 34, 4997-5006, 2000.

Gray C.M., Monson R.K. and Fierer N.: Emissions of volatile organic compounds during the decomposition of plant litter. Journal of Geophysical Research, 115, 2010.

Hayward S., Muncey R.J., James A.E., Halsall C.J. and Hewitt C.N.: Monoterpene emissions from soil in a Sitka spruce forest. Atmospheric Environment, 35, 4081-4087, 2001.

Hayward S., Tani A., Owen S. M. and Hewitt, C.N.: Online analysis of volatile organic compound emissions from Sitka spruce (*Picea sitchensis*). Tree Physiology, 24, 721–728, 2004.

Isebrands J.G., Guenther A.B., Harley P., Helmig D., Klinger L., Vierling L., Zimmerman P. and
Geron C.: Volatile organic compound emission rates from mixed deciduous and coniferous forests in Northern Wisconsin USA. Atmospheric Environment, 33, 2527-2536, 1999.

Jacob D.J., Field B.D., Jin E.M., Bey I., Li Q., Logan J.A. and Yantosca R.M.: Atmospheric budget of acetone. Journal of Geophysical Research, 107, D10, 2002.

Jacob D.J., Field B.D., Li Q., Blake D.R., de Gouw J., Warneke C., Hansel A., Wisthaler A., Singh H.B. Guenther A.: Global budget of methanol: Constraints from atmospheric observations. Journal of Geophysical Research, 110, D08303, 2005.

Jardine K.J., Monson R.K., Abrell L., Saleska S.R., Arneth A., Jardine A., Ishida F.Y., Serrano A.M.Y., Artaxo P., Karl T., Fares S., Goldstein A., Loreto F. and Huxman T.: Within-plant isoprene oxidation confirmed by direct emissions of oxidation products methyl vinyl ketone and methacrolein. Global Change Biology, 18, 973-984, 2012.

Kalogridis C., Gros V., Sarda-Esteve R., Langford B., Loubet B., Bonsang B., Bonnaire N., Nemitz E., Genard A.-C., Boissard C., Fernandez C., Ormeño E., Baisnée D., Reiter I. and Lathière J.: Concentrations and fluxes of isoprene and oxygenated VOCs at a French Mediterranean oak forest. Atmospheric Chemistry and Physics Discussions, 14, 871-917, 2014.

Karl T., Guenther A., Jordan A., Fall R. and Lindinger W.: Eddy covariance measurement of biogenic oxygenated VOC emissions from hay harvesting. Atmospheric Environment, 35, 491-495, 2001.

Karl T.G., Spirig C., Rinne J., Stroud C., Prevost P., Greenberg J., Fall R. and Guenther A.: Virtual disjunct eddy covariance measurements of organic compound fluxes from a subalpine forest using proton transfer reaction mass spectrometry. Atmospheric Chemistry and Physics, 2, 279-291, 2002.

Karl T., Guenther A., Spirig C., Hansel A. and Fall R.: Seasonal variation of biogenic VOC emissions above a mixed hardwood forest in northern Michigan. Geophysical Research Letters, 30, 2186, 2003.

Karl T., Potosnak M., Guenther A., Clark D., Walker J., Herrick J.D. and Geron C.: Exchange processes of volatile organic compounds above a tropical rain forest: Implications for modeling tropospheric chemistry above dense vegetation. Journal of Geophysical Research, 109, D18306, 2004.

Karl T., Harley P., Guenther A., Rasmussen R., Baker B., Jardine K. and Nemitz, E.: The bi-directional exchange of oxygenated VOCs between a loblolly pine (*Pinus taeda*) plantation and the atmosphere. Atmospheric Chemistry and Physics, 5, 3015-3031, 2005.

Karl T.G., Christian T.J., Yokelson R.J., Artaxo P., Hao W.M. and Guenther A.: The tropical forest and fire emissions experiment: method evaluation of volatile organic compound emissions measured by PTR-MS, FTIR, and GC from tropical biomass burning. Atmospheric Chemistry and Physics,7, 8755-8793, 2007.

Karl T., Harley P., Emmons L., Thornton B., Guenther A., Basu C., Turnipseed A. and Jardine K.: Efficient atmospheric cleansing of oxidized organic trace gases by vegetation. Science, 330, 816-819, 2010.

Kaser L., Karl T., Guenther A., Graus M., Schnitzhofer R., Turnipseed A., Fischer L., Harley P., Madronich M., Gochis D., Keutsch F.N. and Hansel A.: Undisturbed and disturbed above canopy ponderosa pine emissions: PTR-TOF-MS measurements and MEGAN 2.1 model results. Atmospheric Chemistry and Physics, 13, 11935-11947, 2013.

Kesselmeier J., Bode K., Gerlach C. and Jork, E.-M.: Exchange of atmospheric formic and acetic acids with trees and crop plants under controlled chamber and purified air conditions. Atmospheric Environment, 32, 1765-1775, 1998.

König G., Brunda M., Puxbaum H., Hewitt C.N., Duckham S.C. and Rudolph J.: Relative contribution of oxygenated hydrocarbons to the total biogenic VOC emissions of selected mid-European agricultural and natural plant species. Atmospheric Environment, 29, 861-874, 1995.

Kuhn U., Rottenberger S., Biesenthal T., Ammann C., Wolf A., Schebeske G., Oliva S.T., Tavares T.M. and Kesselmeier J.: Exchange of short-chain monocarboxylic acids by vegetation at a remote tropical forest site in Amazonia. Journal of Geophysical Research, 107, 8069, 2002.

Kuster W.C., Jobson B.T., Karl T., Riemer D., Apel E., Goldan P.D. and Fehsenfeld F.C.: Intercomparison of volatile organic carbon measurement techniques and data at La Porte during the TexAQS2000 Air Quality Study. Environmental Science & Technology, 38, 221-228, 2004.

Laffineur Q., Aubinet M., Schoon N., Amelynck C., Müller J.-F., Dewulf J., van Langenhove H., Steppe K., Šimpraga M. and Heinesch B.: Isoprene and monoterpene emissions from a mixed temperate forest. Atmospheric Environment, 45, 3157-3168, 2011.

Langford B., Davison B., Nemitz B. And Hewitt C.N.:Mixing ratios and eddy covariance flux measurements of volatile organic compounds from an urban canopy (Manchester, UK). Atmospheric Chemistry and Physics, 9, 1971-1987, 2009.

Langford B., Misztal P.K., Nemitz E., Davison B., Helfter C., Pugh T.A.M., MacKenzie R.M., Lim S.F. and Hewitt C.N.: Fluxes and concentrations of volatile organic compounds from a South-East Asian tropical rainforest. Atmospheric Chemistry and Physics, 10, 8391-8412, 2010a.

Langford B., Nemitz E., House E., Philips G.J., Famulari D., Davison B., Hopkins J.R., Lewis A.C. and Hewitt C.N.: Fluxes and concentrations of volatile organic compounds above central London, UK. Atmospheric Chemistry and Physics, 10, 627-645, 2010b.

Lee A., Goldstein A.H., Keywood M.D., Gao S.,Varutbangkul V., Bahreini R., Ng N.L., Flagan R.C. and Steinfeld J.H.: Gas-phase products and secondary aerosol yields from the ozonolysis of ten different terpenes. Journal of Geophysical Research, 111, D07302, 2006.

Leff J.W. and Fierer N.: Volatile organic compound (VOC) emissions from soil and litter samples. Soil Biology and Biochemistry, 40, 1629-1636, 2008.

Llusià J. and Peñuelas J.: Emission of volatile organic compounds by apple trees under spider mite attack and attraction of predatory mites. Experimental and Applied Acarology, 25, 65-77, 2001.

Llusià J., Peñuelas J. and Gimeno B.S.: Seasonal and species-specific response of VOC emissions by Mediterranean woody plant to elevated ozone concentrations. Atmospheric Environment, 36, 3931-3938, 2002.

Llusià T.M., Müller M., Schnitzhofer R., Karl T., Graus M. Bamberger I., Hörtnagl L., Brilli F., Wohlfahrt G. and Hansel A.: Eddy covariance VOC emission and deposition fluxes above grassland using PTR-TOF. Atmospheric Chemistry and Physics, 11, 611-625, 2011.

Loreto F., Barta C., Brilli F. and Nogues I.: On the induction of volatile organic compound emissions by plants as consequence of wounding or fluctuations of light and temperature, Plant, Cell and Environment, 29, 1820-1828, 2006.

Luecken D.J., Hutzell W.T., Strum M.L. and Pouliot G.A.: Regional sources of atmospheric formaldehyde and acetaldehyde, and implications for atmospheric modelling. Atmospheric Environment, 47, 477-490, 2012.

Maffei M.: Sites of synthesis, biochemistry and functional role of plant volatiles. South African Journal of Botany, 76, 612-631, 2010.

Millet D.B., Jacob D.J., Custer T.G., de Gouw J.A., Goldstein A.H., Karl T., Singh H.B., Sive B.C., Talbot R.W., Warneke C. and Williams J.: New constraints on terrestrial and oceanic sources of atmospheric methanol. Atmospheric Chemistry and Physics, 8, 6887-6905, 2008.

Millet D.B., Guenther A., Siegel D.A., Nelson N.B., Singh H.B., de Gouw J.A., Warneke C., Williams J., Eerdekens G., Sinha V., Karl T., Flocke F., Apel E., Riemer D.D., Palmer P.I., and Barkley M.: Global atmospheric budget of acetaldehyde: 3-D model analysis and constraints from in-situ and satellite observations. Atmospheric Chemistry and Physics, 10, 3405–3425, 2010.

Misztal P.K., Nemitz E., Langford B., Di Marco C.F., Phillips G.J., Hewitt C.N., MacKenzie A.R., Owen S.M., Fowler D., Heal M.R. and Cape J.N.: Direct ecosystem fluxes of volatile organic compounds from oil palms in South-East Asia. Atmospheric Chemistry and Physics, 11, 8995-9017, 2011.

Monks P.S. et al.: Atmospheric composition change – global and regional air quality. Atmospheric Environment, 43, 5268–5350, 2009.

Müller K., Haferkorn S., Grabmer W., Wisthaler A., Hansel A., Kreuzwieser J., Cojocariu C., Rennenberg H. and Herrmann H.: Biogenic carbonyl compounds within and above a coniferous forest in Germany. Atmospheric Environment, 40, 81-91, 2006.

Nemitz E., Hargreaves K.J., Neftel A., Loubet B., Cellier P., Dorsey J.R., Flynn M., Hensen A., Weidinger T., Meszaros R., Horvath L., Dämmgen U., Frühauf C., Löpmeier F.J., Gallagher M.W. and Sutton, M.A.: Intercomparison and assessment of turbulent and physiological exchange parameters of grassland. Biogeosciences, 6, 1445-1466, 2009.

Owen S.M., Boissard C. and Hewitt C.N.: Volatile organic compounds (VOCs) emitted from 40 Mediterranean plant species: VOC speciation and extrapolation to habitat scale. Atmospheric Environment, 35, 5383-5409, 2001.

Park J.-H., Goldstein A.H., Timkovsky J., Fares S., Weber R., Karlik J., and Holzinger R.: Active atmosphere-ecosystem exchange of the vast majority of detected volatile organic compounds. Science, 341, 643-647, 2013.

Paulot F., Wunch D., Crounse J.D., Toon G.C., Millet D.B., DeCarlo P.F., Vigouroux C., Deutscher N.M., González Abad G., Notholt J., Warneke T., Hannigan J.W., Warneke C., de Gouw J.A., Dunlea E.J., De Mazière M., Griffith D.W.T., Bernath P., Jimenez J.L. and Wennberg P.O.: Importance of secondary sources in the atmospheric budgets of formic and acetic acids. Atmospheric Chemistry and Physics, 11, 1989-2013, 2011.

Peñuelas J., Filella I., Stefanescu C. and Llusià J.: Caterpillars of Euphydryas aurinia (*Lepidoptera: Nymphalidae*) feeding on *Succisa pratensis* leaves induce large foliar emissions of methanol. New Phytologist, 167, 851-857, 2005.

Pérez-Rial D., Peñuelas J., López-Mahía P. and Llusià J.: Terpenoid emissions from *Quercus robur*. A case study of Galicia (NW Spain). Journal of Environmental Monitoring, 11, 1268-1275, 2009.

Pier P.A.: Isoprene emission rates from Northern Red Oak using a whole-tree chamber. Atmospheric Environment, 29, 1347-1353, 1995.

Pinto D.M., Blande J.D., Nykänen R., Dong W.-X., Nerg A.-M. and Holopainen J.K.: Ozone degrades common herbivore-induced plant volatiles: does this affect herbivore prey location by predators and parasitoids? Journal of Chemical Ecology, 33, 683-694, 2007.

Riemer, D., Pos W., Milne P., Farmer C., Zika R., Apel E., Olszyna K., Kliendienst T. Lonneman W., Bertman S., Shepson P. and Starn T.: Observations of nonmethane hydrocarbons and oxygenated volatile organic compounds at a rural site. Journal of Geophysical Research, 103, 28111-28128, 1998.

Rinne J., Ruuskanen T.M., Reissell A., Taipale R., Hakola H. and Kulmala M.: On-line PTR-MS measurements of atmospheric concentrations of volatile organic compounds in a European boreal forest ecosystem. Boreal Environment Research, 10, 425-436, 2005.

Rinne J., Taipale R., Markkanen T., RuuskanenT.M., Hellén H., Kajos M.K., VesalaT., and Kulmala M.: Hydrocarbon fluxes above a Scots pine forest canopy: measurements and modelling. Atmospheric Chemistry and Physics, 7, 3361–3372, 2007.

Rottenberger S., Kuhn U., Wolf A., Schebeske G., Oliva S.T., Tavares T.M. and Kesselmeier J.: Formaldehyde and acetaldehyde exchange during leaf development of the Amazonian deciduous tree species Hymenaea courbaril. Atmospheric Environment, 39, 2275-2279, 2005.

Ruuskanen T.M., Müller M., Schnitzhofer R., Karl T., Graus M., Bamberger I., Hörtnagl L., Brilli F., Wohlfahrt G. and Hansel A.: Eddy covariance VOC emission and deposition fluxes above grassland using PTR-TOF. Atmospheric Chemistry and Physics, 11, 611–625, 2011.

Scutareanu P., Bruin J., Posthumus M.A. and Drukker B.: Constitutive and herbivore-induced volatiles in pear, alder and hawthorn trees. Chemoecology, 74, 63-74, 2003

Schade G.W. and Goldstein A.H.: Fluxes of oxygenated volatile organic compounds from a ponderosa pine plantation. Journal of Geophysical Research, 106, 3111-3123, 2001

Schade G.W. and Goldstein A.H.: Seasonal measurements of acetone and methanol: Abundances and implications for atmospheric budgets. Global Biogeochemical Cycles, 20, GB1011, 2006

Seco R., Peñuelas J. and Filella I.: Short-chain oxygenated VOCs: Emission and uptake by plants and atmospheric sources, sinks, and concentrations. Atmospheric Environment, 41, 2477-2499, 2007

Singh H.B., Kanakidou M. Crutzen P.J. and Jacob D.J.: High concentrations and photochemical fate of oxygenated hydrocarbons in the global troposphere. Nature, 378, 50-54, 1995

Spirig C., Neftel A., Ammann C., Dommen J., Grabmer W., Thielmann A., Schaub A., Beauchamp J., Wistthaler A. And Hansel A.: Eddy covariance flux measurements of biogenic VOCs during ECHO 2003 using proton transfer reaction mass spectrometry. Atmospheric Chemistry and Physics, 5, 465-481, 2005

Staudt M., Wolf A. and Kesselmeier J.: Influence of environmental factors on the emissions of gaseous formic and acetic acids from orange (Citrus sinensis L.) foliage. Biogeochemistry, 48, 199-216, 2000

Taipale R., Ruuskanen T.M. and Rinne J.: Lag time determination in DEC measurements with PTR-MS. Atmospheric Measurement Techniques, 3, 853-862, 2010

Tarvainen, V., Hakola, H., Hellén, H., Bäck, J., Hari, P. and Kulmala, M.: Temperature and light dependence of the VOC emissions of Scots pine. Atmospheric Chemistry and Physics, 5, 989-998, 2005

Tie X., Guenther A. and Holland E.: Biogenic methanol and its impacts on tropospheric oxidants. Geophysical Research Letters, 30, 2003

von Dahl C.C., Hävecker M., Schlögl R. and Baldwin I.T.: Caterpillar-elicited methanol emission: a new signal in plant–herbivore interactions? The Plant Journal, 46, 948–960, 2006

Warneke C., Karl T., Judmaier H., Hansel A., Jordan A., Lindinger W. and Crutzen P.J.: Acetone, methanol and other partially oxidized volatile organic emissions from dead plant matter by abiological processes: Significance for atmospheric HOx chemistry. Global Biogeochemical Cycles, 13, 9-17, 1999

Wienhold F.G., Frahm H. and Harris G.W.: Measurements of N_2O fluxes from fertilized grassland using a fast response tunable diode laser spectrometer. Journal of Geophysical Research, 99, 16557-16567, 1994

Winters A.J., Adams M.A., Bleby T.M., Rennenberg H., Steigner D., Steinbrecher R. and Kreuzwieser J.: Emissions of isoprene, monoterpene and short-chained carbonyl compounds from Eucalyptus spp. in southern Australia. Atmospheric Environment, 43, 3035-3043, 2009